Measuring Dispersal and Tracking of Anti-Icing and Deicing Chemicals by Using In-Situ Spectral Data Phase II

FINAL PROJECT REPORT

by

Nathan Belz | University of Alaska Fairbanks
Gabriel Fulton | University of Alaska Fairbanks

DISCLAIMER

The contents of this report reflect the views of the authors, who are responsible for the facts and the accuracy of the information presented herein. This document is disseminated under the sponsorship of the U.S. Department of Transportation's University Transportation Centers Program, in the interest of information exchange. The Pacific Northwest Transportation Consortium, the U.S. Government and OSU, UI, UAF, UW, and WSU assume no liability for the contents or use thereof.

Technical Report Documentation Page

1. Report No.	2. Government Accession No. 01701498	3. Recipient's Catalog No.	
4. Title and Subtitle Measuring Dispersal and Tracking of Anti-Icing and Deicing Chemicals by Using In-Situ Spectral Data – Phase II		**5. Report Date**	
		6. Performing Organization Code G00010259	
7. Author(s) Nathan Belz | University of Alaska Fairbanks Gabriel Fulton | University of Alaska Fairbanks		**8. Performing Organization Report No.** 2018-S-UAF-2	
9. Performing Organization Name and Address PacTrans Pacific Northwest Transportation Consortium University Transportation Center for Region 10 University of Washington More Hall 112 Seattle, WA 98195-2700		**10. Work Unit No. (TRAIS)**	
		11. Contract or Grant No. 69A3551747110	
12. Sponsoring Organization Name and Address United States of America Department of Transportation Research and Innovative Technology Administration		**13. Type of Report and Period Covered** Final Report, 09/2018 – 09/2019	
		14. Sponsoring Agency Code	
15. Supplementary Notes Report uploaded at www.pacTrans.org			

16. Abstract

The use and application of salt, sand and related mixtures and derivatives have proved to be highly effective for removing or controlling the development of ice on the roadway surface. Although ample research has indicated the way in which application method, application rate, and efficacy of mix contents can vary depending on temperature and surface conditions, little if any research has looked at the longevity and dispersal of anti-icing and deicing compounds after they have been applied to the roadway surface (i.e., how long it stays in place and where it goes post-application). This research extended a lab-based methodology developed in the UAF Hyperspectral Lab, in which spectroscopy was used to measure concentrations of anti-icing and deicing chemicals, into a field setting. Results showed both the promise of using imaging spectroscopy for winter maintenance and management, particularly for beet-brine solutions, and some limitations associated with environmental and roadway surface conditions.

17. Key Words Winter maintenance, remote sensing, spectrometry, anti-icing, deicing		18. Distribution Statement No restrictions.	
19. Security Classification (of this report) Unclassified.	**20. Security Classification (of this page)** Unclassified.	**21. No. of Pages** 50	**22. Price** N/A

Form DOT F 1700.7 (8-72) **Reproduction of completed page authorized**

SI* (MODERN METRIC) CONVERSION FACTORS

APPROXIMATE CONVERSIONS TO SI UNITS

Symbol	When You Know	Multiply By	To Find	Symbol
		LENGTH		
in	inches	25.4	millimeters	mm
ft	feet	0.305	meters	m
yd	yards	0.914	meters	m
mi	miles	1.61	kilometers	km
		AREA		
in^2	square inches	645.2	square millimeters	mm^2
ft^2	square feet	0.093	square meters	m^2
yd^2	square yard	0.836	square meters	m^2
ac	acres	0.405	hectares	ha
mi^2	square miles	2.59	square kilometers	km^2
		VOLUME		
fl oz	fluid ounces	29.57	milliliters	mL
gal	gallons	3.785	liters	L
ft^3	cubic feet	0.028	cubic meters	m^3
yd^3	cubic yards	0.765	cubic meters	m^3
	NOTE: volumes greater than 1000 L shall be shown in m^3			
		MASS		
oz	ounces	28.35	grams	g
lb	pounds	0.454	kilograms	kg
T	short tons (2000 lb)	0.907	megagrams (or "metric ton")	Mg (or "t")
		TEMPERATURE (exact degrees)		
°F	Fahrenheit	5 (F-32)/9 or (F-32)/1.8	Celsius	°C
		ILLUMINATION		
fc	foot-candles	10.76	lux	lx
fl	foot-Lamberts	3.426	candela/m^2	cd/m^2
		FORCE and PRESSURE or STRESS		
lbf	poundforce	4.45	newtons	N
lbf/in^2	poundforce per square inch	6.89	kilopascals	kPa

APPROXIMATE CONVERSIONS FROM SI UNITS

Symbol	When You Know	Multiply By	To Find	Symbol
		LENGTH		
mm	millimeters	0.039	inches	in
m	meters	3.28	feet	ft
m	meters	1.09	yards	yd
km	kilometers	0.621	miles	mi
		AREA		
mm^2	square millimeters	0.0016	square inches	in^2
m^2	square meters	10.764	square feet	ft^2
m^2	square meters	1.195	square yards	yd^2
ha	hectares	2.47	acres	ac
km^2	square kilometers	0.386	square miles	mi^2
		VOLUME		
mL	milliliters	0.034	fluid ounces	fl oz
L	liters	0.264	gallons	gal
m^3	cubic meters	35.314	cubic feet	ft^3
m^3	cubic meters	1.307	cubic yards	yd^3
		MASS		
g	grams	0.035	ounces	oz
kg	kilograms	2.202	pounds	lb
Mg (or "t")	megagrams (or "metric ton")	1.103	short tons (2000 lb)	T
		TEMPERATURE (exact degrees)		
°C	Celsius	1.8C+32	Fahrenheit	°F
		ILLUMINATION		
lx	lux	0.0929	foot-candles	fc
cd/m^2	candela/m^2	0.2919	foot-Lamberts	fl
		FORCE and PRESSURE or STRESS		
N	newtons	0.225	poundforce	lbf
kPa	kilopascals	0.145	poundforce per square inch	lbf/in^2

*SI is the symbol for the International System of Units. Appropriate rounding should be made to comply with Section 4 of ASTM E380.
(Revised March 2003)

TABLE OF CONTENTS

List of Figures

List of Tables

List of Abbreviations

AKDOT&PF   Alaska Department of Transportation and Public Facilities

Band math   Mathematical comparison of wavelengths

HyLab   Hyperspectral Imaging Laboratory

MDSS   Maintenance decision support system

NaCl   Sodium chloride

NDVI   Normalized Difference Vegetation Index

NIR   Near infrared

PDA   Personal digital assistant

PSR+   PSR+ 3500 Spectroradiometer

RWIS   Remote weather information systems

USDOT   United States Department of Transportation

Acknowledgments

CHAPTER 1. Introduction

1.1. Problem Statement

The management of anti-icing and deicing efforts is critical for traveler mobility and safety (Kuemmel and Hanbali, 1992) during winter seasons in cold climates. The statewide cost of a winter road closure has been estimated to be an average of $700 million per day (IHS, 2015). The use and application of salt, sand, gravel, and related derivatives have proved to be highly effective for removing or controlling the development of ice on the roadway surface. A considerable amount of research has looked at the way in which application methods, application rates, and efficacy of mix contents can vary depending on temperature and surface conditions. Substantial research has also been conducted on the environmental impacts to soil and groundwater of anti-icing and deicing applications, as well as the corrosive properties of different types of chlorides. However, little if any research has looked at the longevity and dispersal of anti-icing and deicing compounds after they have been applied to the roadway surface (i.e., how long they stay in place and where they go post-application). It stands to reason that anti-icing and deicing compounds (e.g., salt and sand) are only effective at or above a certain concentration. That is to say, if the amount of salt in solution becomes too dilute, then it no longer has the capacity to control the development of ice or melt it on the roadway. The research presented here sought to fill that knowledge gap.

1.2. Background

Obtaining robust measurements to quantify the rate of loss of deicing and anti-icing chemicals with manual methods would be time and cost prohibitive, and obtaining spatially representative samples would be difficult over long time periods. To that end, this research evaluated a laboratory-proven methodology by which spectroscopy can be used to measure

concentrations of anti-icing and deicing chemicals. Imaging spectroscopy, also known as hyperspectral imaging, is an advanced remote sensing technology that allows wavelength measurements to be taken from a distance. The technology uses sophisticated sensors that can scan and generate hundreds of images of any surface-based target material. These images are used together to reconstruct the unique pattern in which the material reflects energy, thereby allowing for accurate identification.

In Phase I of this project (Belz and Fulton, 2019), sample materials were acquired from the Alaska Department of Transportation & Public Facilities (AKDOT&PF) to construct lab samples of varying concentrations of brine, aggregate, carbohydrate additive, and water (figure 1.1). Preliminary hyperspectral imaging laboratory-based measurements were collected for calibration and validation purposes from a range of surfaces. Visual inspection shows that these surfaces in a field setting are quite different from each other (figure 1.2).
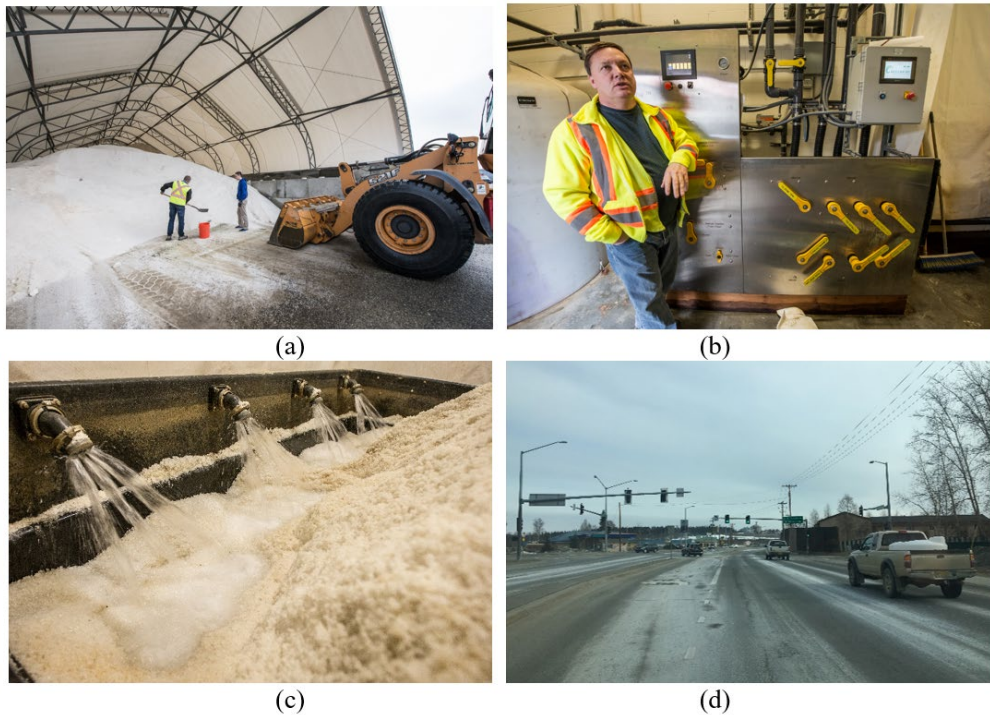

(a)　　　　　　　　　　　　　　(b)

(c)　　　　　　　　　　　　　　(d)

Figure 1.1. Examples of (a) acquired DOT material (salt shown), (b,c) the anti-icing mixing process, and (d) applied anti-icing material on a highway in Fairbanks, Alaska.
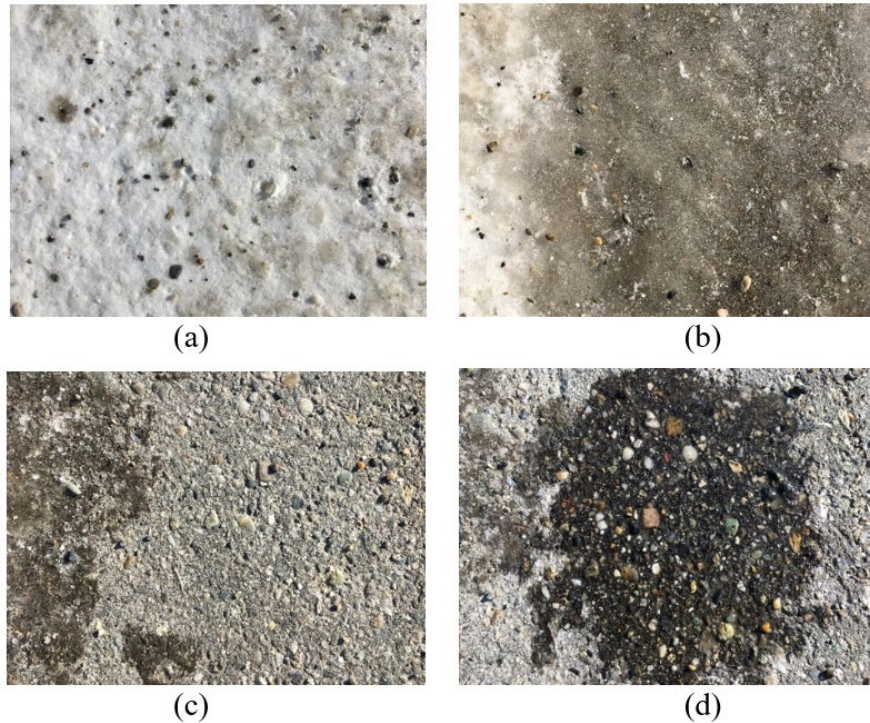
Figure 1.2. Example surface materials showing (a) hard-packed snow with some gravel, (b) partially melted hard-pack with some ice, (c) bare pavement with some ice, and (d) pavement with wet brine added.

1.3. Research Need

Ideally, this research will lead to the development of integrated spectrometer units that can be collocated with remote weather information systems (RWIS) stations, thus allowing them to be used in conjunction with a maintenance decision support system (MDSS). The MDSS assists maintenance personnel in the decision-making processes of determining roadway maintenance activities by providing real-time and post-storm analysis to evaluate materials used, rates of application, and timing of application (Fay et al., 2015). A study conducted in Indiana found that by using an MDSS, the salt savings in the winter of 2008 were about 228,470 tons at a cost of $12,108,910, and if normalized for winter conditions based on storm severity, the total salt savings were 188,274 tons at a cost of $9,978,536 (McClellan et al., 2009). Reducing salt usage while also maintaining safe roads is a keen interest of those who utilize salt for winter

maintenance purposes. The benefits of information gathering and processing are demonstrated by increased safety and cost savings.

1.4. Objectives

The objectives of this Phase II were threefold. First, develop a robust in-field sampling plan to measure anti-icing and deicing chemical concentrations under varied environmental, geometric, and volumetric conditions. Second, conduct the field data collection. Third, develop and conduct a sampling strategy to quantify the amount of anti-icing and deicing chemical loss due to imposed processes. Lastly, use these findings to inform and improve winter maintenance efforts and strategies.

Chapter 2. Data and Methods

<u>4.2</u>   <u>2.1 Field Sample Preparation</u>

In the lab setting used in Phase 1, most aspects of the experiment could be regulated and kept constant (e.g., light source and intensity, angle of light, sources of lighting or reflectance interference, background continuity, and material concentration). In the field, many of these factors change on a day to day or even an hour by hour basis. Because of these changing features, steps were taken in the procedure to minimize the severity and impact of these factors, which also limited the times and frequency with which samples could be obtained. To satisfy the need for limited atmospheric interference due to cloud coverage (figure 2.1), the thickness of the atmosphere penetrated by sunlight, the angle of sunlight, and ambient air temperature, the appropriate time frames for data collection were limited to as little as a couple hours per week.

(a)   (b)

Figure 2.1 Example of ideal testing condition with (a) clear skies and non-ideal conditions with (b) cloudy skies

The reason for prioritizing days with no cloud cover was that cloud cover is a form of interference that can block, or at least obfuscate, key wavelength reflectance values and possibly reduce or eliminate wavelength pairs that would otherwise reveal key relationships for the sodium chloride and beet juice mixtures. To achieve the best possible consistency, data gathering

was restricted to days with clear skies to avoid unnecessary scattering due to cloud coverage and snowfall. In addition, periods of the day when the sun was near its zenith were avoided to not confound the data with angles of sunlight prone to atmospheric interference. Two backgrounds were used for field testing regularly traveled pavement in a poor state and regularly traveled pavement in well-maintained state. Poorly maintained conditions were defind as white hardpack present on the surface, while well-maintained conditions were defined as minimal ice or snow coverage. The clear ice coverage, asphalt pavement, and hardpack surfaces allowed much thinner volumetric applications to be applied than during lab testing. Liquid doses as miniscule as 0.5 mL could be applied with a perfume spray bottle to ensure complete coverage. Well maintained pavement conditions were defined as having a clearly visible, near-dry asphalt surface.

The final location for field testing was a primary aisle in a parking lot on the University of Alaska, Fairbanks (UAF) campus. This location satisfied the greatest number of criteria for a winter roadway (a location with a background of asphalt pavement, driven on repeatedly by vehicles, plowed, with a clear line of sight to the sun, and easy access) without fully requiring closure of a road or obstructing traffic flow (see figure 2.2).

Figure 2.2 Testing conditions with (a) hardpack present and (b) hardpack removed to simulate a well-maintained road.

The parking lot had some notable issues to address to obtain data representative of traveled winter roadways. The most obvious problem was the amount of snow or ice found on the surface. Unlike most roads actively treated with deicer, the parking lot was not plowed completely to the asphalt surface. The parking lot could accumulate hardpack as thick as 2 inches in some locations, which was not an accurate representation of roads regularly treated with deicer, even in the poorest conditions. Our solution was to mechanically remove hardpack (figure 2.2b) and to pour boiling water to melt it down to surface asphalt layer. If the excavated location smelled of petroleum/oil or showed physical signs of other foreign material being present, a new location was selected to minimize possible contaminants that could affect the analysis.

4.3   2.2 Instrumentation

Setting up the PSR+ 3500 Spectroradiometer (PSR+) hyperspectral unit required steps identical to those for data collection in the lab (Belz and Fulton, 2019), apart from the added steps of securing the hyperspectral unit into a carrying backpack and connecting the included personal digital assistant (PDA) unit to the hyperspectral unit via Bluetooth for remote activation

7

and data storage. Solutions (mixtures of brine and beet-brine deicers) were fabricated using an identical procedure to lab solutions. Details regarding material type, temperature, cloud coverage, time, and artifacts were recorded by hand in a field book. After data collection has been completed, all data from the PDA were extracted via USB and stored locally on the lab computer.

4.4   2.3 Field Data Collection

To ensure that each constituent was adequately represented, a reference panel was used to calibrate the PSR+ unit and the background. This background reflectance was then used to calibrate the reading based on interference (see figure 2.3).
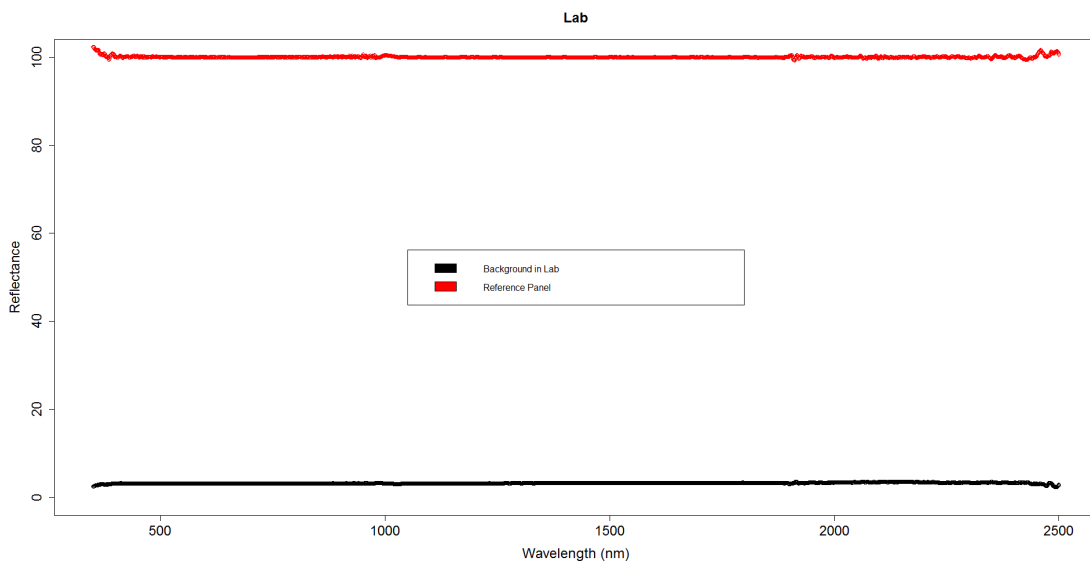

Figure 2.3 Lab reference panel and lab background

The noise generated from the reference panel demonstrated the accuracy of the PSR+ spectrometer with near perfect accuracy from the 1000-nm wavelength to the 1900-nm wavelength. Even at the edges of the spectrum recordable by the unit, the PSR+ had a 1 percent accuracy range except for a few unique points, as shown in figure 2.4. In the figure, the red lines

represent standard deviation and show uncertainty due to either artifacts, ambient changes, or
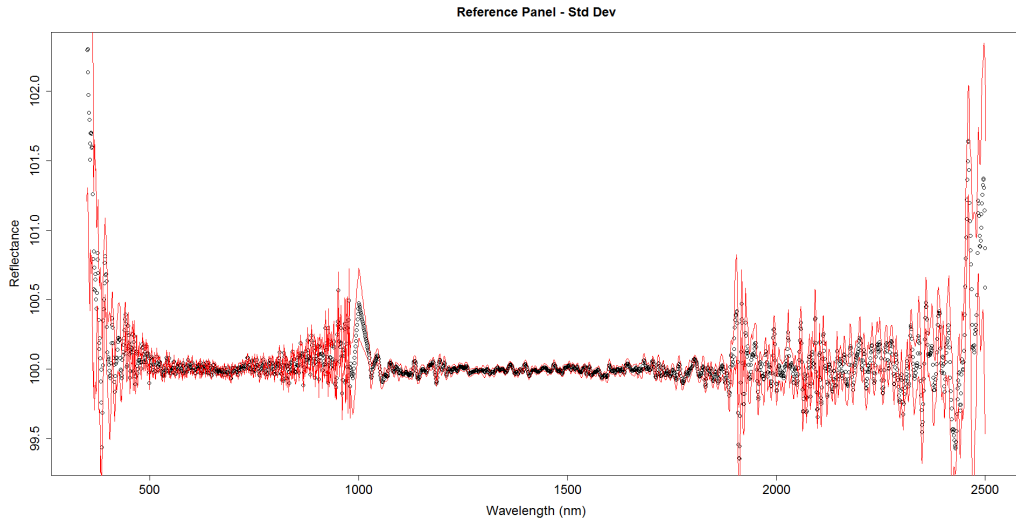
material changes.

Figure 2.4 Reference panel referencing accuracy

For comparison, the background material under which the liquid materials were obtained

in Phase I was an extremely muted black matte painted plyboard. The curve itself sat at about 3.2

percent reflectance so as to not interfere with the reflectance produced by the measured targets

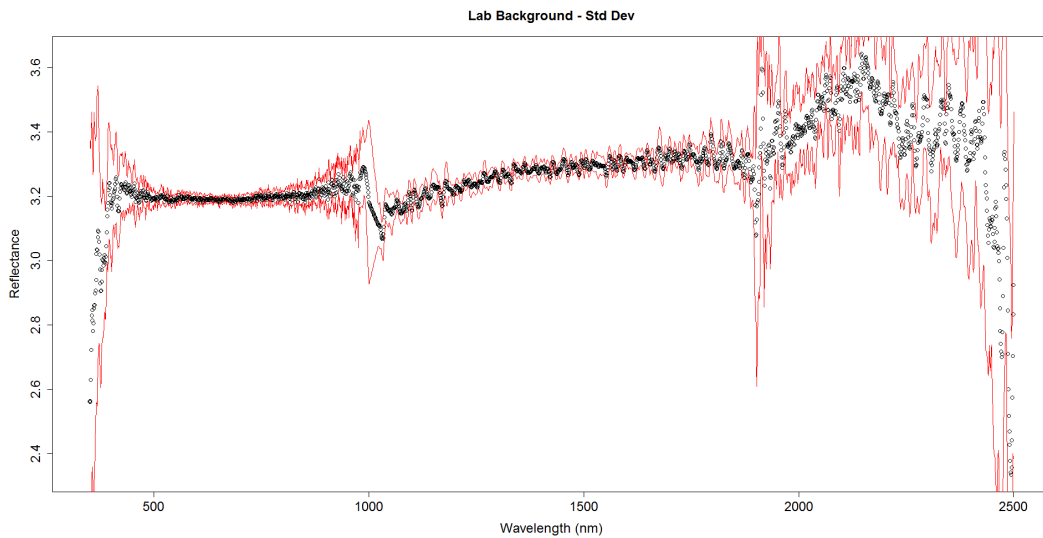and produced small standard deviations, typically under 1 percent (figure 2.5).

Figure 2.5 Lab background reflectance

Delineation of the test area in the field was achieved by using a metal collar with a 6-inch diameter to limit the amount of material spread across the pavement surface and to reduce the amount of chemical solution needed in the experiment. Assuming chemical application at a rate of 30 to 50 gallons per lane mile, as documented by AKDOT&PF, and 11-ft lanes, the rates for field applications rates and volumes were computed as shown in table 2.1.

Table 2.1 Field volumetrics

Applied (mL)	NaCl (%)	NaCl (mg)	Area (cm²)	Conc. (mg/cm²)	Conc. (gal/lane mile)
0.5	5	25	182.41	0.14	8.38
1	5	50	182.41	0.27	16.77
5	5	250	182.41	1.37	83.85
10	5	500	182.41	2.74	167.69
Applied (mL)	NaCl (%)	NaCl (mg)	Area (cm²)	Conc. (mg/cm²)	Conc. (gal/lane mile)
0.5	10	50	182.41	0.27	16.77
1	10	100	182.41	0.55	33.54
5	10	500	182.41	2.74	167.69
10	10	1000	182.41	5.48	335.38
Applied (mL)	NaCl (%)	NaCl (mg)	Area (cm²)	Conc. (mg/cm²)	Conc. (gal/lane mile)
0.5	15	75	182.41	0.41	25.15
1	15	150	182.41	0.82	50.31
5	15	750	182.41	4.11	251.54
10	15	1500	182.41	8.22	503.08
Applied (mL)	NaCl (%)	NaCl (mg)	Area (cm²)	Conc. (mg/cm²)	Conc. (gal/lane mile)
0.5	23.3	116.5	182.41	0.64	39.07
1	23.3	233	182.41	1.28	78.14
5	23.3	1165	182.41	6.39	390.72
10	23.3	2330	182.41	12.77	781.45

Liquid doses at 0.5 mL were applied with a perfume spray bottle to ensure complete coverage. For the remainder of the application rates, testing solutions were applied with 1-mL syringe or 5-mL graduated cylinder and were spread mechanically with a rinsed rubber glove to ensure complete surface coverage. Applications exceeding AKDOT&PF application rates resulted in chemical migration from the test area. This migration was controlled by implementing

a physical barrier in the form of non-hardening rope caulk. The caulk proved to be effective at lower concentrations but showed limited success at the highest application volumes tested, and the efficacy diminished as the time from initial application increased. All brine concentrations were repeated with appropriate beet-brine concentrations as if the solution had been diluted from a 23.3 percent brine solution that had been mixed at a ratio of 80:20 brine to beet juice.

Chapter 3 Analysis

3.1 Data Characteristics

Because collecting spectral data in the field proved to be more dynamic than collecting data in the lab (with a high dependence on referencing because of atmospheric interference and subtle changes in the lighting environment), slight changes in reflectance were expected for the samples taken in the field as a result of changes in cloud cover and changes in light angle over time. However, these slight changes in reflectance value were not expected to alter the overall shape of the reflectance curve. Comparing a measurement under poor conditions (see figure 3.1a) to ideal conditions (see figure 3.1b) confirmed that noise increased as lighting conditions deteriorated. That is, variance was magnified under cloudy conditions. However, the trend, valleys, peaks, and relative magnitude remained the same, which are the main vectors used in band math analysis.

Another change introduced by field conditions was a background that changed for each set of samples. Asphalt pavement replaced the static matte black background. These winter roadway backgrounds, while quite uniform to the human eye, were not equivalent to the spectral imaging and band math analysis. One sample site utilized for testing is illustrated in figure 3.2, in which test sites are labeled with numbers corresponding to the order of shot acquisition.

13

Reference Panel - cloudy

(a)

Reference Panel - clear
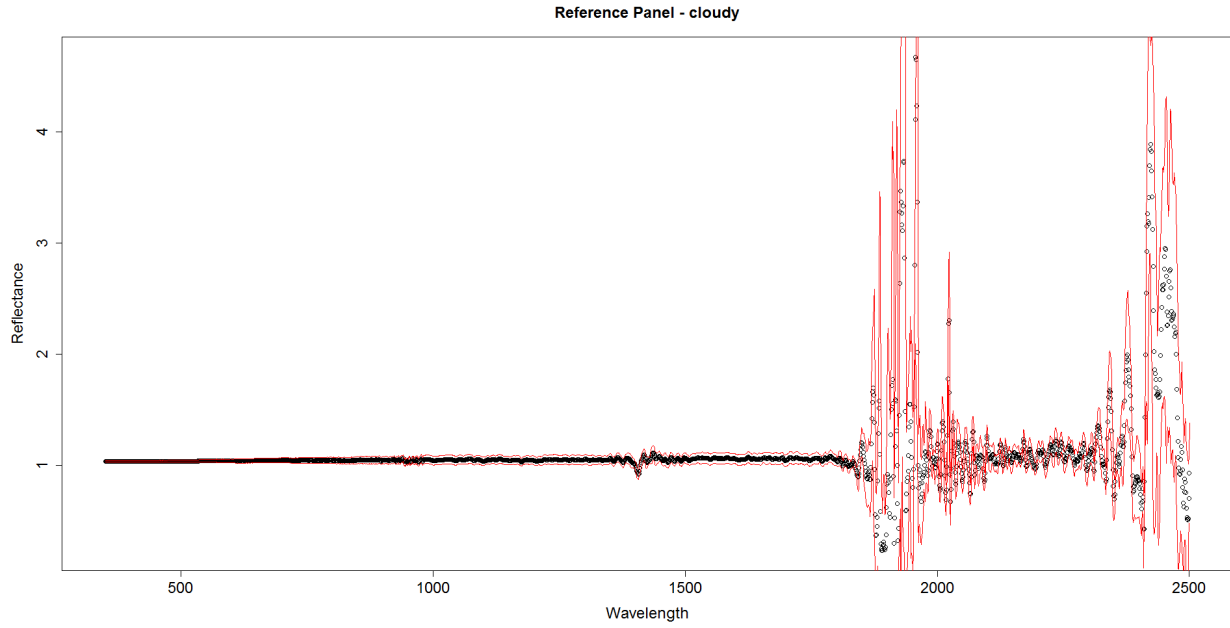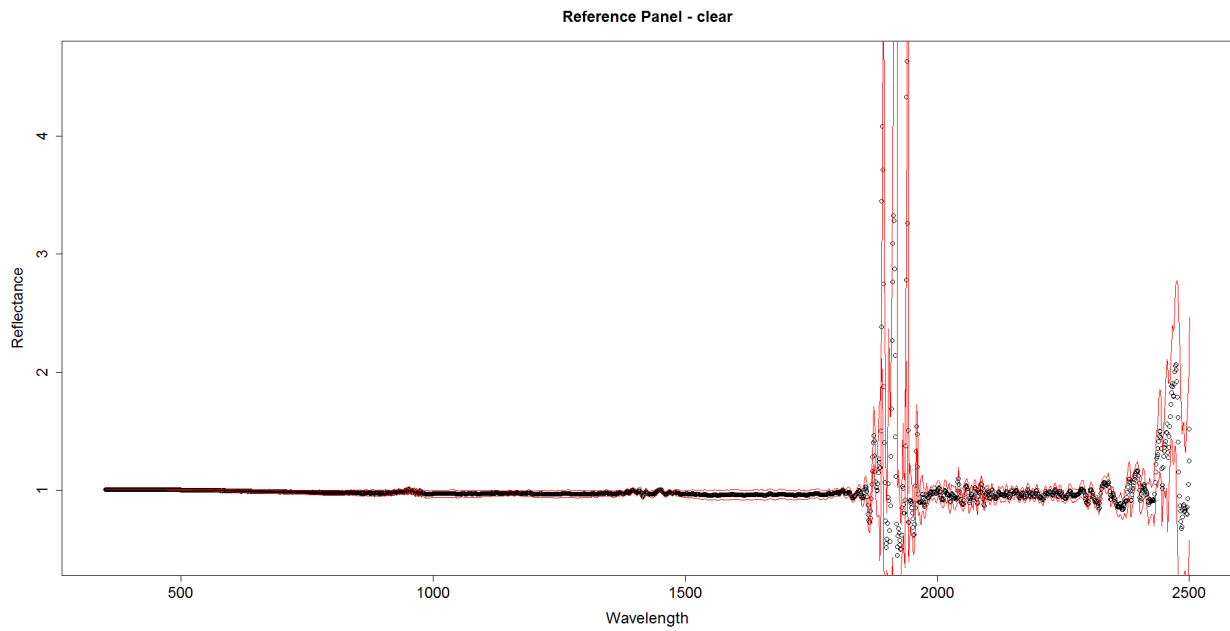
(b)

Figure 3.1 Coverage effects of a (a) cloudy sky and (b) clear sky

Figure 3.2 Example test site with rope caulk barriers

4.6   3.2 Brine Comparisons

The first step in the field data analysis was to record the "backgrounds" before the deicing material was applied. The reflectance curves of well-maintained asphalt pavement with light icing is shown in figure 3.3.
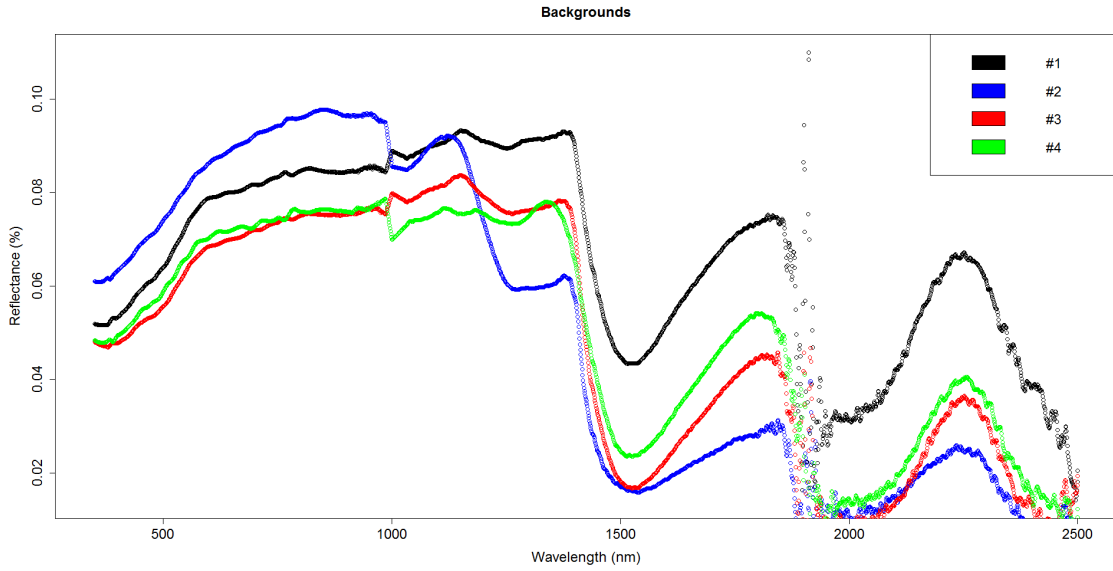
Figure 3.3 Field, background reflectance curves

In the figure, the background curves have significant differences in reflectance magnitudes at certain portions of the curve. The shapes of the background curves are similar; however, there are severe deviances around the 1000-nm wavelength and the 1250-nm wavelength. The differences established in the background material were still present after deicing chemicals had been applied (shown in figure 3.4).
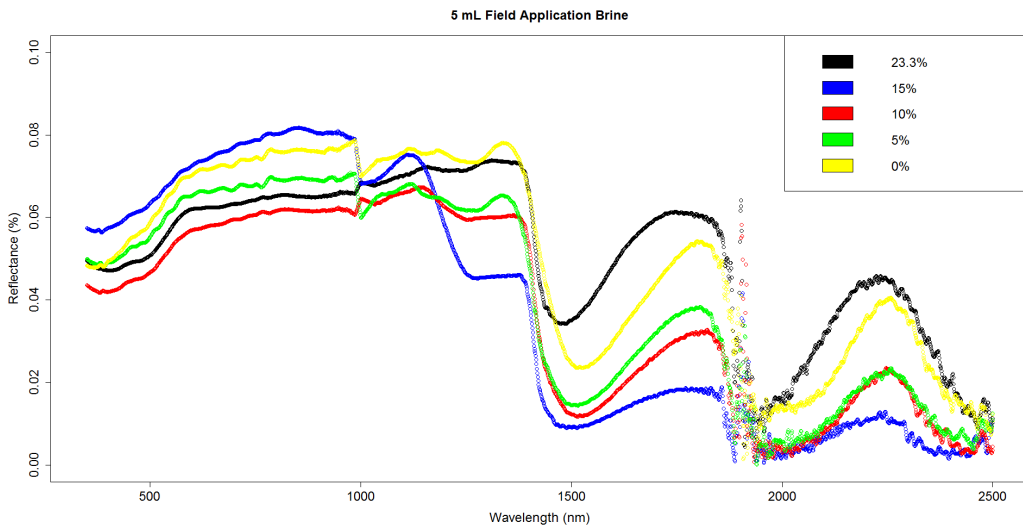

Figure 3.4 Field, changing salt concentrations

The difference in magnitude made linear comparison between the curves challenging. In order to account for variations in background and the associated effects on reflectance curves, all chemical application reflectance values were divided by their respective background before deicing solutions were applied. The results are shown in figure 3.5.
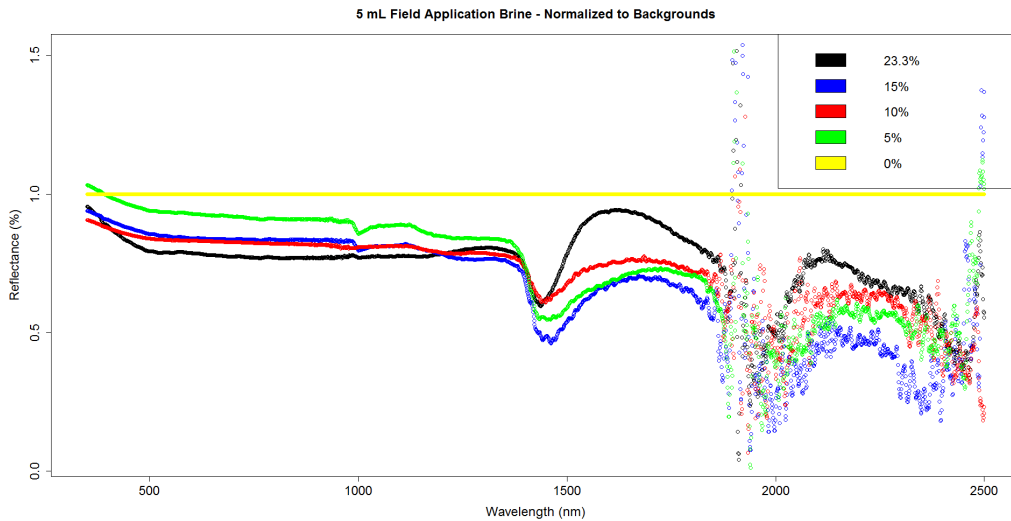

Figure 3.5 Field changing salt concentrations, normalized to the background

Normalizing by the respective backgrounds helped to define the degradation due to scatter and uncertainty; wavelength values that exceeded 1800 nm became incredibly scattered. Even with normalization, no obvious relationships between concentration and reflectance values could be observed. The procedure for each application site was to apply deicing material of a specified concentration at numerous volumetric applications. To eliminate the variance due to significant changes in background reflectance, curves of constant concentration were compared while the volumetric application rate was changed.

Once background variation had been controlled for, trends in reflectance values became more apparent. The most visually significant, ranging from the 1450-nm to 1800-nm wavelengths, exhibited significant changes in magnitude as volumes changed (see figure 3.6).
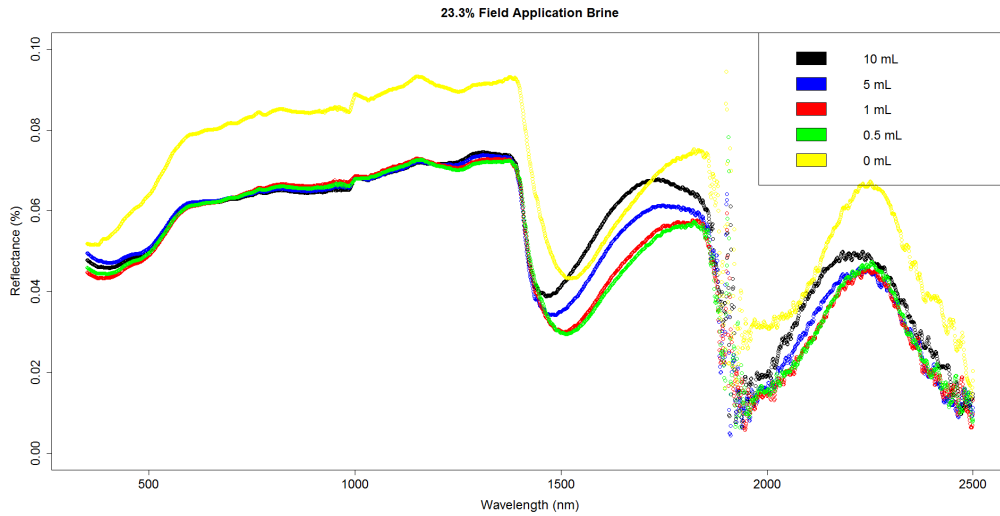
17

Figure 3.6 Brine-changing volumes, constant concentration

The differences between reflectance patterns for backgrounds merely inches apart illustrated the significant effects that changes in road background can make, with points being nearly double the value simply because of slight changes in ice surface coverage (see figure 3.3). Ideally, a small cluster of shots on a well-maintained asphalt pavement would have near equal reflectance values when analyzed. Analysis of variance for a background analysis would ideally indicate no statistically significant difference, but the analysis shown in figure 3.7 indicated a large difference.
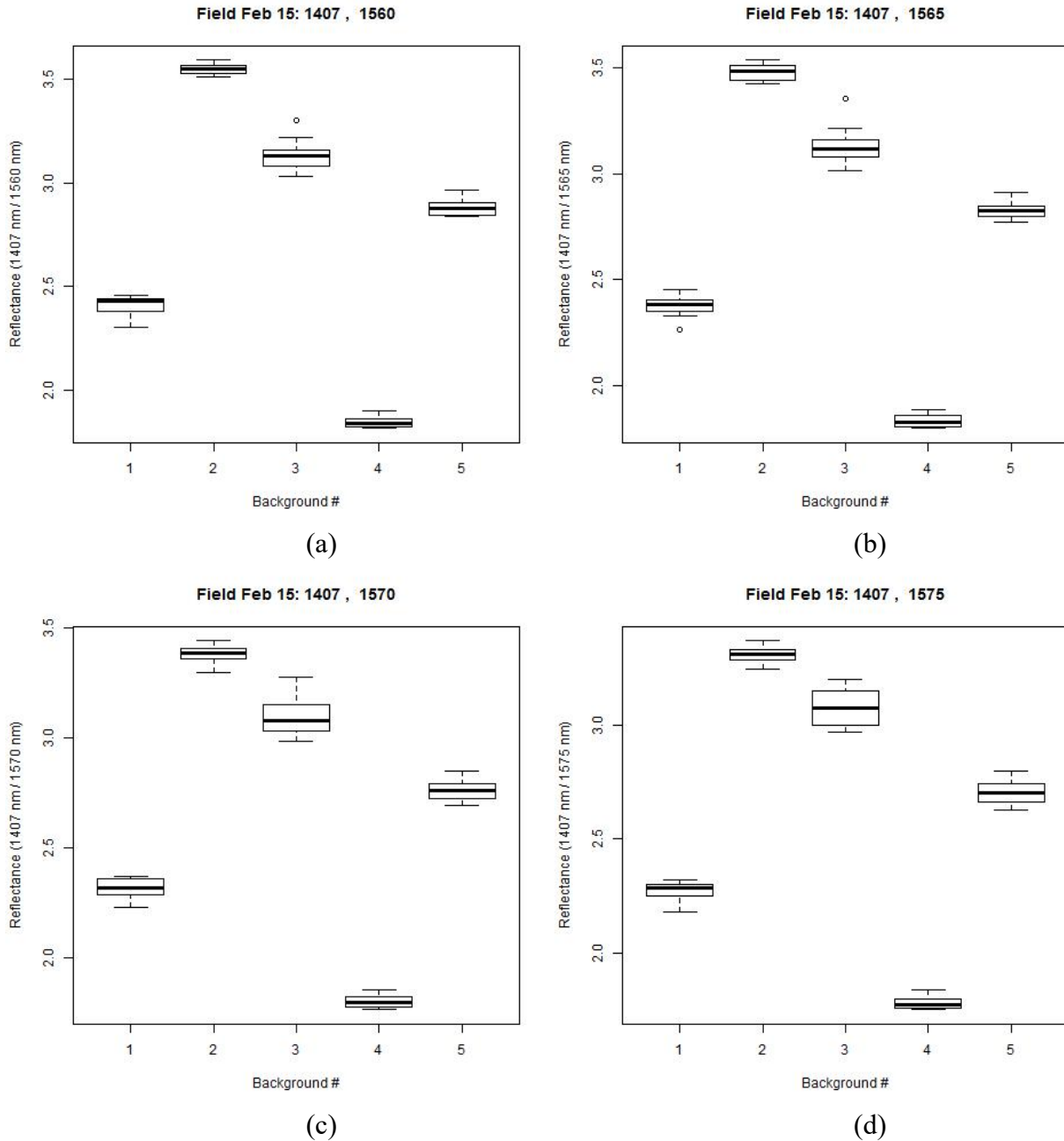
Figure 3.7 Good condition asphalt pavement background with varied wavelength pairs to 1407 nm (a) 1560 nm through (d) 1575 nm

An ANOVA test (table 3.1) showed that there was a significant difference between the testing sites, even though the sites were close in proximity and had similar surface features. The pairwise comparison (table 3.2) confirmed that all points were statistically significantly different

from one another and suggested that different concentrations of deicing compounds might be identifiable by using band math equations.

Table 3.1 Analysis of variance table (1407 nm, 1575 nm)

Values	Df	Sum Sq.	Mean Sq.	F value	Pr(>F)
ind	4	12.8843	3.2211	936.08	<2.2e-16 ***
Residuals	45	0.1548	0.0034	-	-

Table 3.2 Pairwise comparisons (1407 nm, 1575 nm)

Background #	1	2	3	4
2	<2e-16	-	-	-
3	3.70E-12	7.00E-04	-	-
4	9.40E-14	<2e-16	3.80E-13	-
5	2.30E-13	5.30E-15	7.80E-08	<2e-16

4.7   Beet-Brine Comparisons

As with the brine deicing solutions, the varied backgrounds underlying the beet-brine solutions caused offset and disruption, as demonstrated by the lack of a visually linear trend as deicing concentrations changed shown in figure 3.8.
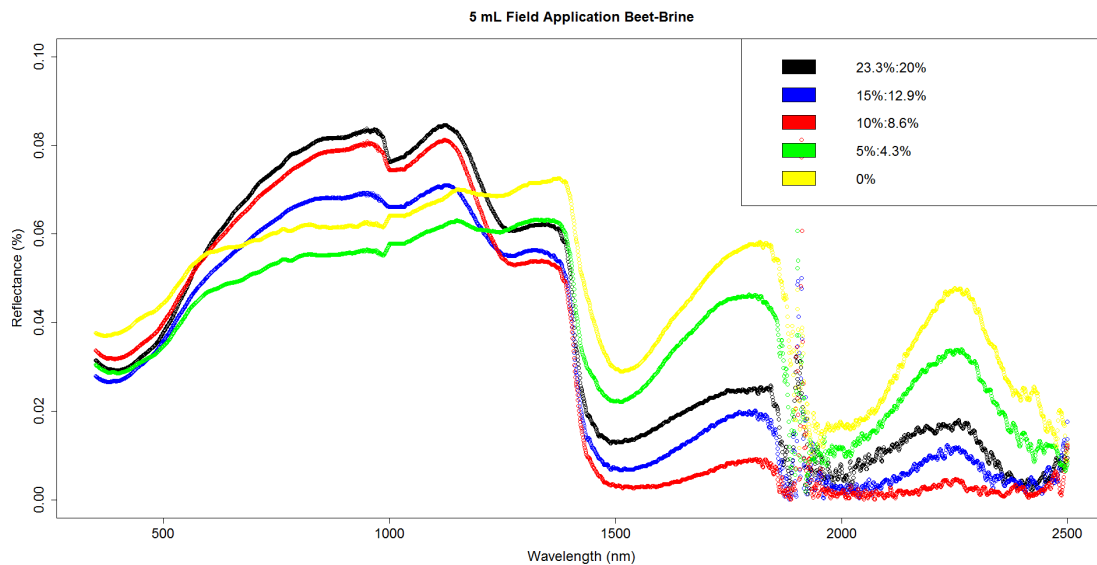

Figure 3.8 Beet-brine concentrations based on field data

A possible remedy for the varied backgrounds was to normalize each concentration to the appropriate surface layer underlying the applied deicer, as shown in figure 3.9.
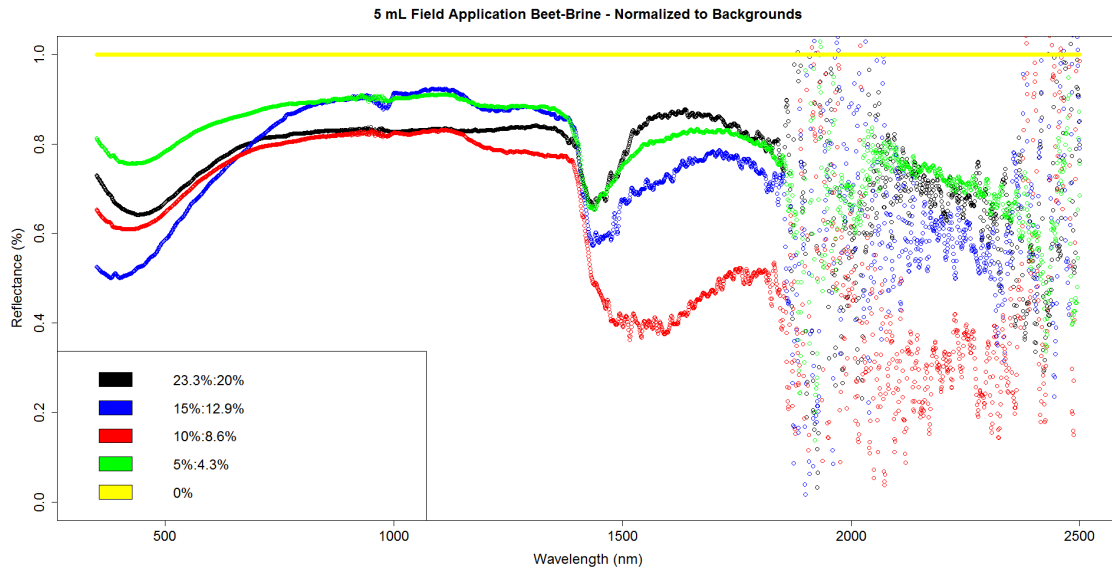

Figure 3.9 Field, changing beet-brine concentrations, normalized to the background

As with the brine deicer, most of the data were obliterated as wavelength values exceeded 1800 nm. Additionally, there were strong deviations around the 1400-nm wavelength. However, the curves did not appear to be great indicators of changing deicer presence. As with the brine deicer testing, the procedure for each application site was to apply deicing material of a specified concentration at numerous volumetric applications. To eliminate the variance due to significant changes in background reflectance, the curves of constant concentrations at differing volumetric application rates on the surface of the test site were compared (see figure 3.10).
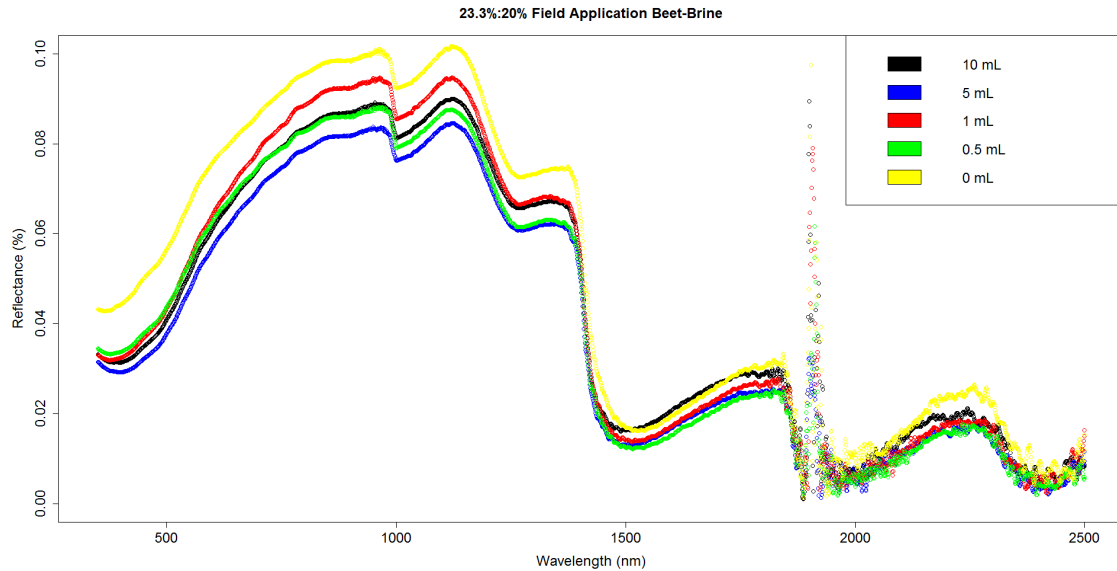
Figure 3.10 Beet-brine, changing volumes, constant concentrations

For most of the curve, there appeared to be no visually linear trend as volumes increased. However, in looking at isolated segments of the spectral curve, such as the visual range, there appeared to be a semi-continuous trend from the 0-mL application to the 5-mL application levels. The lack of continuation at the 10-mL application level may have resulted from material migration at higher volumes. Some migration was also noticed at the 5-mL application level and was inherent to the deicing capabilities of the test materials (i.e., the deicer melted some of the native frozen material and then carried a portion of the deicer material away from the test location). Presumably, the lack of continuity in the relative changes in spectra were a result of this migration.

4.8   Additional Considerations

For the two prime constituents (beet juice and sodium chloride), several different wavelengths were identified as important signifiers of material presence. However, the number of points and frequency and reliability of occurrence for the beet signifiers far outweighed those

of the brine signifiers. The beet signifiers even had the possibility of overwhelming or drowning out some of the brine signifiers deeper in the near infrared (NIR) reflectance range.

For brine solutions, the wavelengths that experienced the most significant change in thickness were in the NIR wavelength range. This was problematic because of the distortion in the NIR reflectance caused by absorption of NIR wavelengths by water. Regardless, several sets of wavelengths were found to be reliable signifiers of changes in salt concentration in the lab setting. With temperature, lighting, and concentrations controlled for, trends were found for 3.6-mm-thick brine solutions in the 2000-nm wavelength; trends occurred for an overwhelming 871 repetitions at the 2120-nm wavelength, and scattered linear relationships occurred at the late 1200-nm wavelengths. For 1.6-mm-thick brine solutions there was no longer a strong outlier; however, there was very strong coverage scattered throughout the 1400-nm to 1600-nm wavelengths with over 1000 repetitions. For 0.8-mm-thick brine solutions the best signifiers of changing salt concentration were focused in the low 1400-nm wavelengths, with a maximum of 111 repetitions. The identification of points for salt concentration as film thickness decreased proved to be a significant indicator and of great interest for this phase of the study. Of the 111 repetitions tested, the majority were adjacent to each other, creating a large portion of a curve that could be sampled and compared to the low 1400-nm wavelengths for more thorough and precise testing. The analysis in Phase 1 produced only four wavelength pairs centered near the 1820-nm wavelength and the 1555-nm wavelength. These points were also used in the analysis of the field data.

For beet carbohydrate, the changes that were maximized were quite different from those of the colorless brine solutions. Red beet carbohydrate is visually distinct. Adding beet juice greatly changes the color of the liquid film, and the greatest changes denoted in the spectral

imaging results are in the visual spectrum. For 3.6-mm-thick beet solutions, the most common points determined to have a linear relationship with concentration changes were in the 600-nm and 1600-nm wavelengths. In comparison to about 75 percent of the recorded spectra, the 600-nm wavelength successfully identified changes in concentration. The results of the 3.6-mm beet film thicknesses were mimicked by the 1.6-mm thickness, with the key difference that most common wavelengths shifted to the mid-600-nm wavelengths instead of the low 600-nm wavelengths. However, in looking at the low 600-nm wavelengths directly, the data revealed that the numbers of repetitions for the wavelengths in the 3.6-mm film slightly increased rather than decreasing as expected. For the 0.8-mm beet thickness, the most repeated wavelengths again shifted inside the visual spectrum, down to the 400-nm wavelengths. This shift was much more significant, and since the 0.8-mm thickness was closest to what would be experienced on actual winter roadways, the wavelengths gathered from it would be the ones most expected to be reliable field indicators. As a final comparison, the differences regardless of film thickness were tested. The resulting values again showcased the low 400-nm wavelengths, with very little loss in repetition, and a decrease from a maximum of 1400 repetitions to 1200 repetitions, which is promising for field applications.

For beet-brine mixtures, the visually significant beet signature far outweighed the much less significant brine signatures. In addition, the spectral signatures for beet-brine mixtures was extremely similar to those of the beet solutions without the salt. The main difference for this mixture was seen in the 3.6-mm and 1.6-mm beet-brine solutions, in which the wavelengths that experienced the greatest change in concentration were located in the mid-500-nm range. Very little difference in beet-brine wavelengths was seen between the 3.6-mm and 1.6-mm thickness, with most pairs around the mid-500-nm wavelengths. Analyzing the 0.8-mm thicknesses showed

relationships nearly identical to those of the beet solutions, with a small range in the low 400-nm wavelengths but a slightly smaller number of repetitions, close to about 100 fewer repetitions on average. The similarities continued with the final comparison of all beet-brine regardless of film thickness; most of the values found in the 0.8-mm beet brine thickness were repeated, thereby being very similar to the beets' 0.8-mm film thickness and the comparison regardless of film thicknesses. A key section of wavelengths to consider will be the 400-nm wavelengths for any concentration involving beet juice. In conclusion, many of the signifiers for beet were present in beet-brine, but some of the brine signifiers actaully dissappeared, suggesting that brine monitoring and identification would be much harder in the field than beet identification.

Chapter 4 Results

4.9   4.1   Brine

To account for the effects of the dynamic backgrounds on reflectance ratio values, the recorded concentrations and volumetric brine applications were normalized by their respective backgrounds obtained before application. The 0.5-mL application, equivalent to 8.4 to 39.1 gallons per lane-mile and most representative of AKDOT&PF application rates, is depicted in figure 4.1.

An ANOVA test comparing 1407 nm to 1560 nm showed that there was a statistically significant effect from changing the concentration of deicing compound at the $p < 0.05$ level for five concentrations [$F(4,45) = 55.72$, $p < 0.001$] at the 1-ml application level (figure 4.2). Conducting a pairwise comparison using t-tests showed that all the different concentrations were statistically significantly different except for the 5 percent brine and 10 percent brine $(p = 0.11)$. The 1-mL applications were equivalent to 16.8 to 78.1 gal/lane-mile in terms of AKDOT&PF liquid brine application.

An ANOVA test comparing 1407 nm to 1560 nm showed that there was a statistically significant effect from changing the concentration of deicing compound at the $p < 0.05$ level for five concentrations [$F(4,45) = 133.03$, $p < 0.001$] at the 5-ml application level (figure 4.3). Conducting a pairwise comparison using t-test showed that all the different concentrations were statistically significantly different. There appeared to be no significant trend, beyond the 23.3 percent application having a lower band math total than the original value.
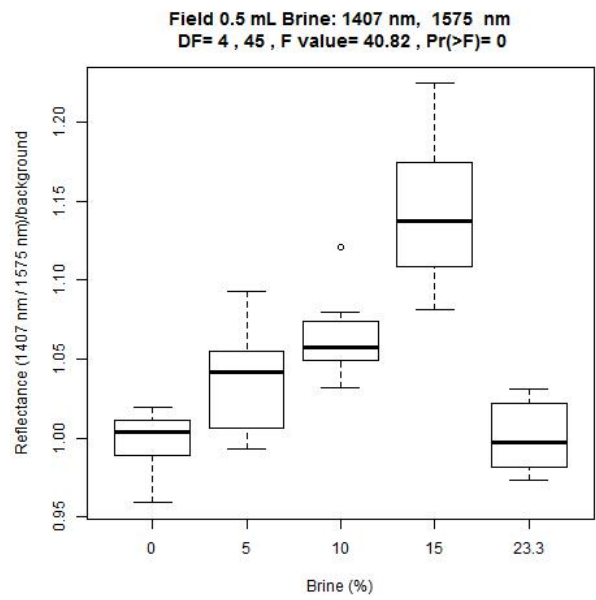
Field 0.5 mL Brine: 1407 nm, 1560 nm
DF= 4 , 45 , F value= 55.72 , Pr(>F)= 0

(a)

Field 0.5 mL Brine: 1407 nm, 1565 nm
DF= 4 , 45 , F value= 48 , Pr(>F)= 0

(b)

Field 0.5 mL Brine: 1407 nm, 1570 nm
DF= 4 , 45 , F value= 39.77 , Pr(>F)= 0

(c)

Field 0.5 mL Brine: 1407 nm, 1575 nm
DF= 4 , 45 , F value= 40.82 , Pr(>F)= 0
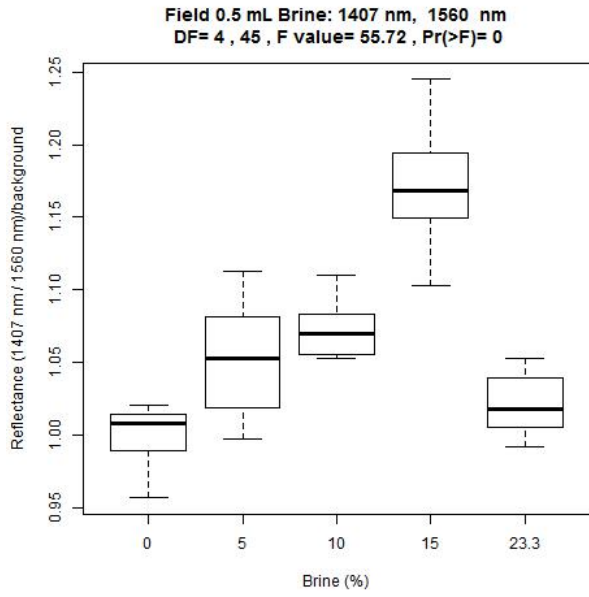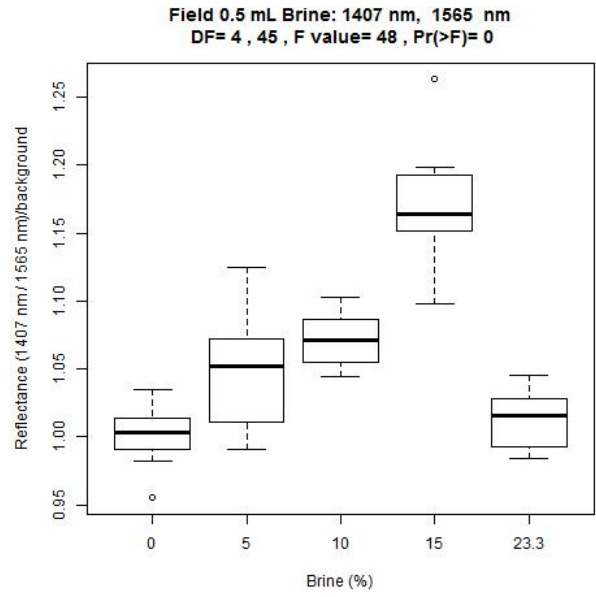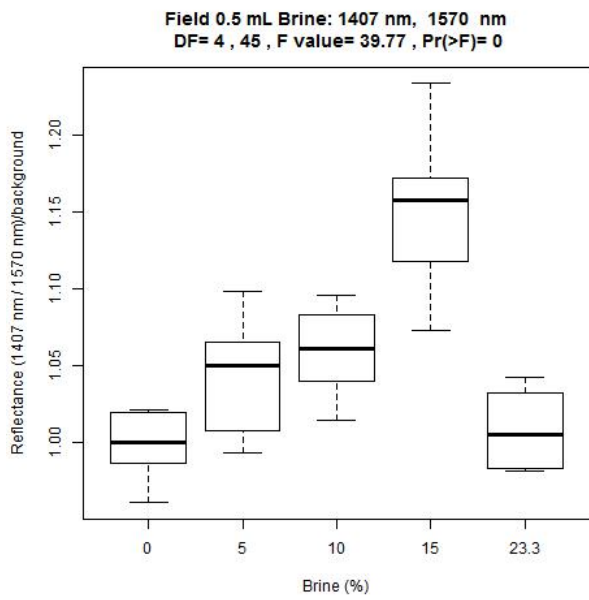
(d)

Figure 3.1 Beet-brine, changing volumes, constant concentrations

(a)

(b)

(c)

(d)
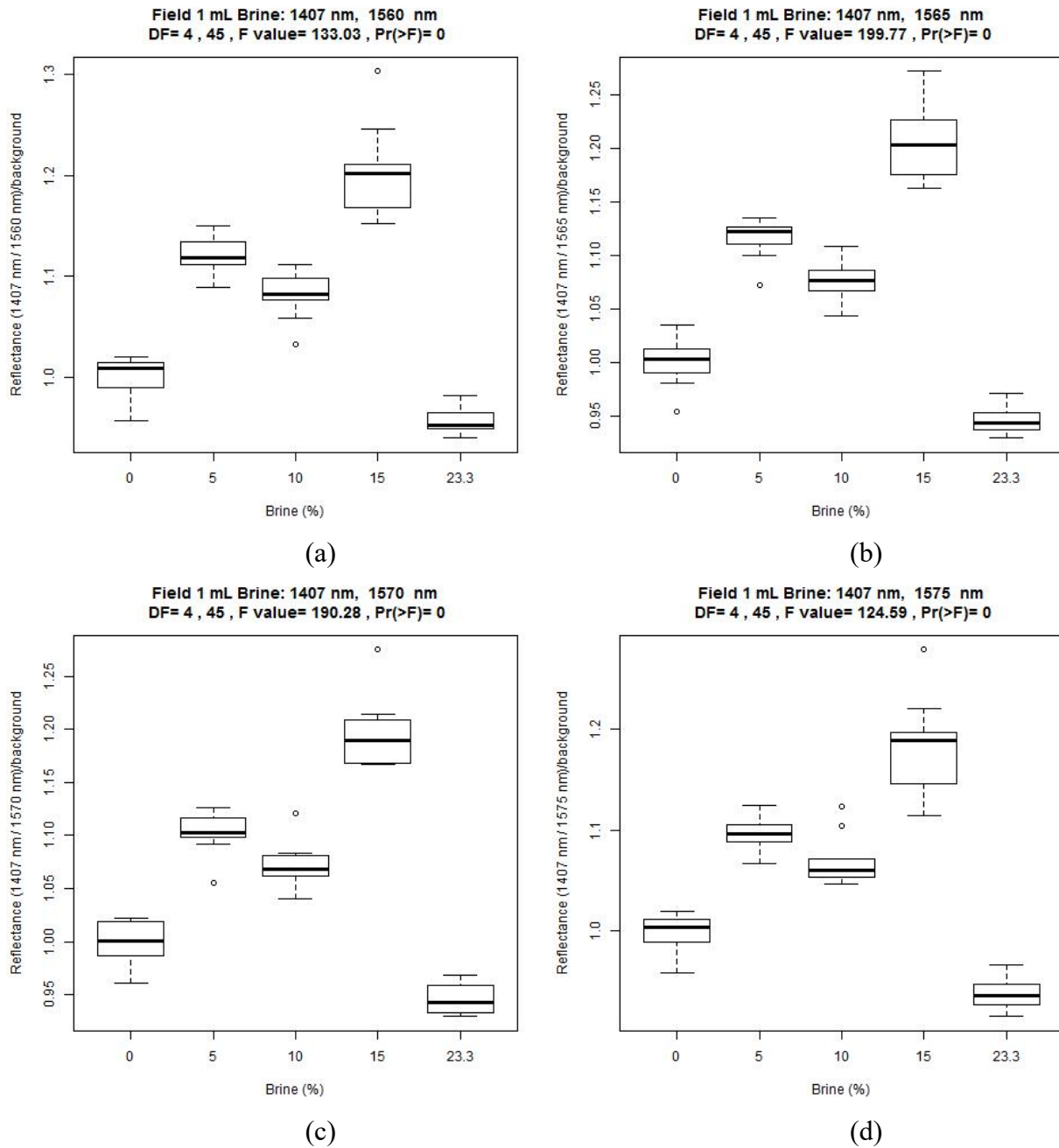
Figure 4.2 1-mL application, field well-maintained pavement (a) through (d)

(a)

(b)

(c)

(d)
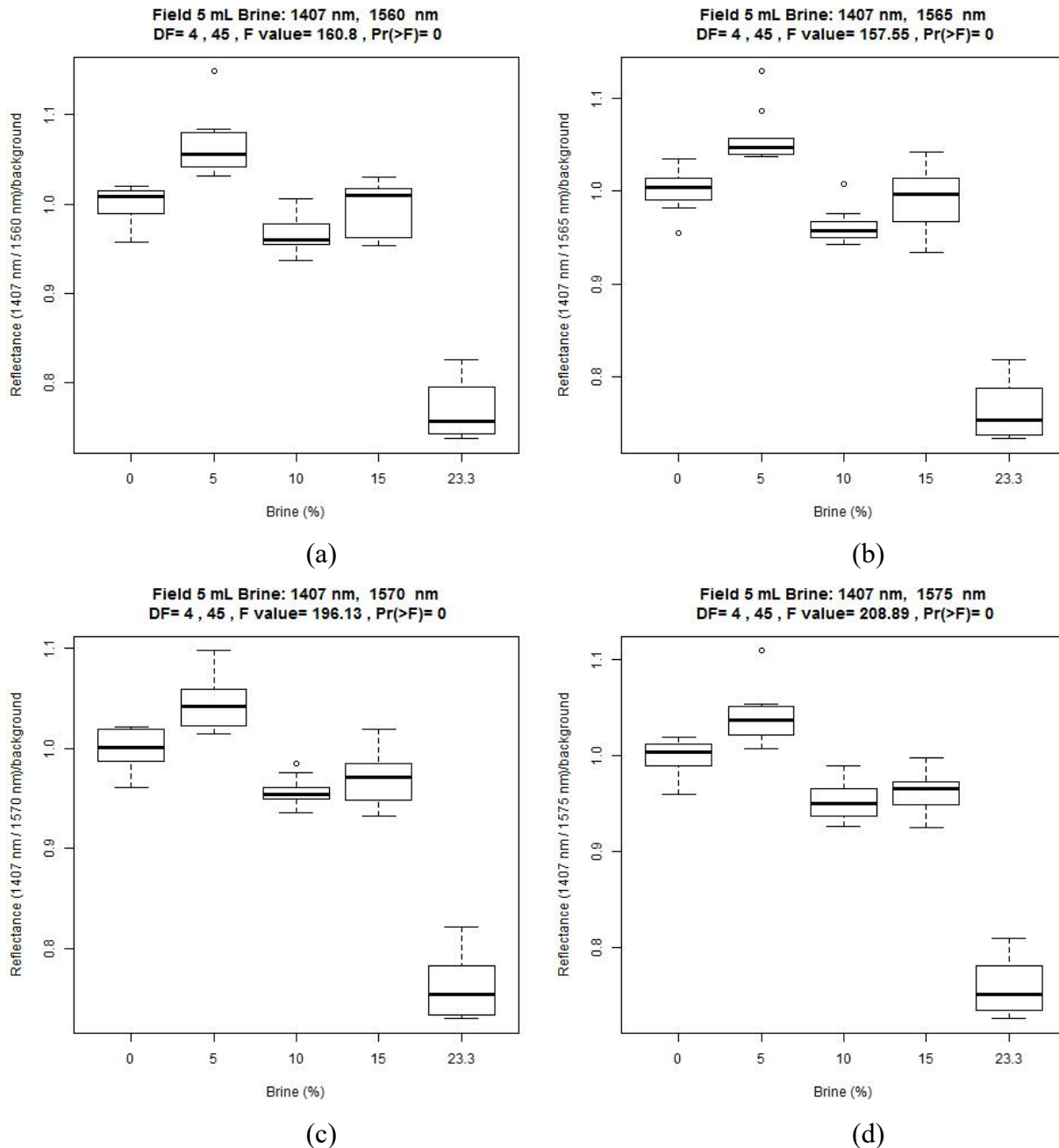
Figure 4.3 5-mL application, field well-maintained pavement (a) through (d)

An ANOVA test comparing 1407 nm to 1560 nm showed that there was a statistically significant effect from changing the concentration of deicing compound at the *p < 0.05* level for five concentrations [F(4,45) = 160.8, *p < 0.001*] at the 10-ml application level. Conducting a pairwise comparison with t-tests showed that all the different concentrations were statistically

significantly different, except for the 0 percent brine in comparison to the 15 percent brine compound with $p = 0.65$. This relationship more closely mimicked what was observed in the lab, and there appeared to be a noticeable drop in band math value in transitioning from 5 percent to 10 percent, with an even more significant drop in transitioning from 15 percent to 23.3 percent.

An ANOVA test comparing 1407 nm to 1560 nm showed that there was a statistically significant effect from changing the concentration of deicing compound at the $p < 0.05$ level for five concentrations [$F(4,45) = 530.11$, $p < 0.001$]. Conducting a pairwise comparison with t-tests showed that all the different concentrations were statistically significantly different, except for the 10 percent brine in comparison to the 15 percent brine compound with a $p = 0.96$. Figure 4.4 shows that there was a significant change in transitioning from 5 percent to 10 percent brine, practically no change from 10 percent to 15 percent, and another significant change from 15 percent to 23.3 percent. Comparing concentrations at different volumes would eliminate the need for normalizing to separate backgrounds, as all applications would have the same background. Ideally these trends would follow the changing salt amounts demonstrated in the lab trials and would eliminate the dynamic backgrounds found in the field.

An ANOVA test comparing 1407 nm to 1560 nm showed that there was a statistically significant effect from changing the concentration of deicing compound at the $p < 0.05$ level for five concentrations [$F(4,45) = 71.64$, $p < 0.001$]. Conducting a pairwise comparison with t-tests showed that all the different concentrations were statistically significantly different, apart from the 0.5-mL 5 percent brine in comparison to the 5-mL 5 percent brine compound with a $p = 0.48$. The 5 percent comparison (as seen in figure 4.5) showed a much more promising relationship between changing salt presence and reflectance value. However, the trend line had a positive slope rather than a negative slope, as demonstrated by the lab data. The trend then visibly

returned to an intuitive negative value when concentrations of greater than 5 percent were
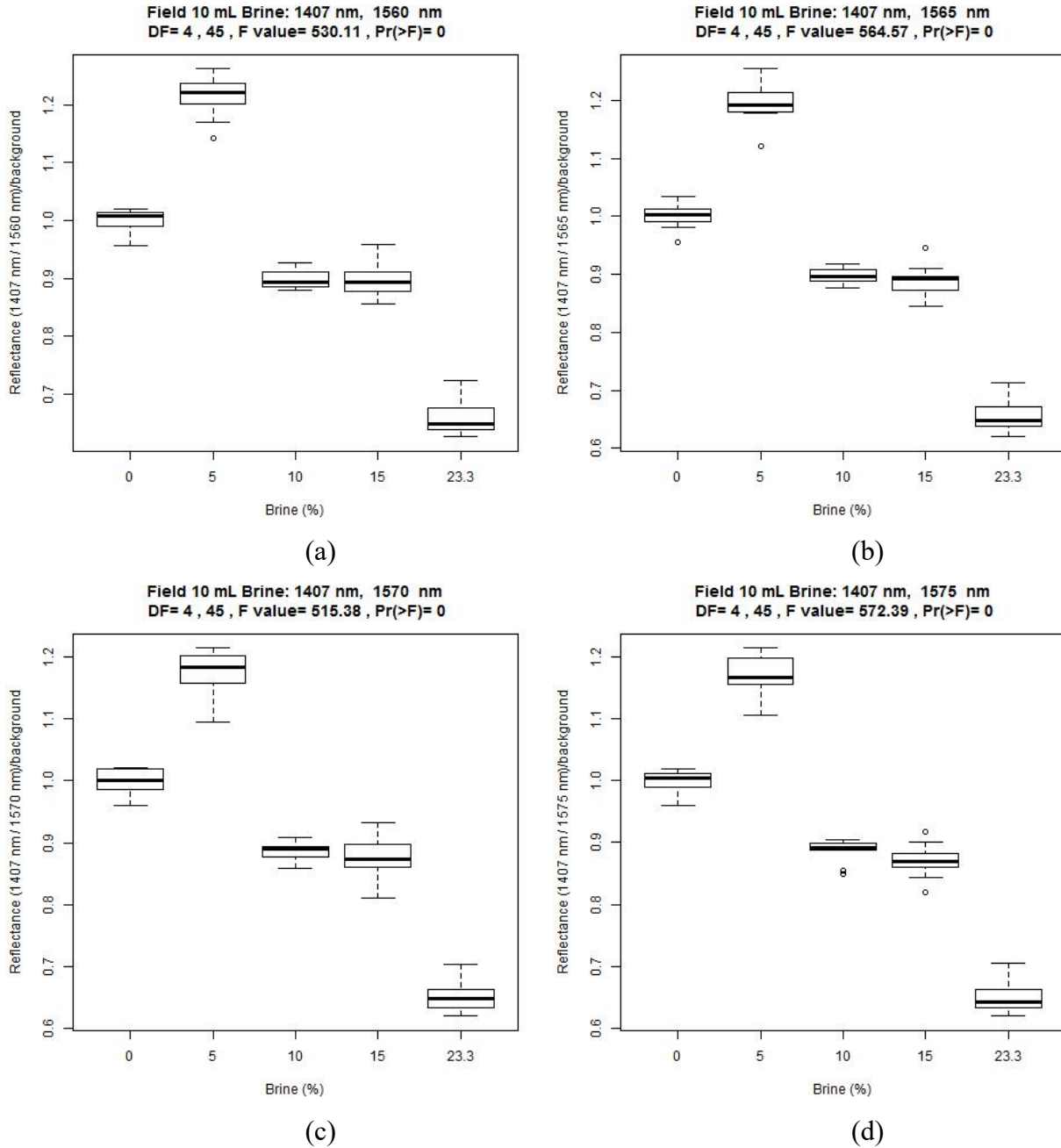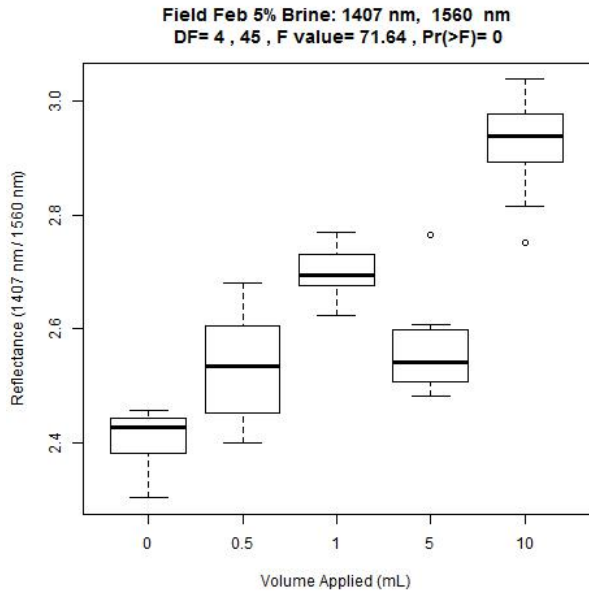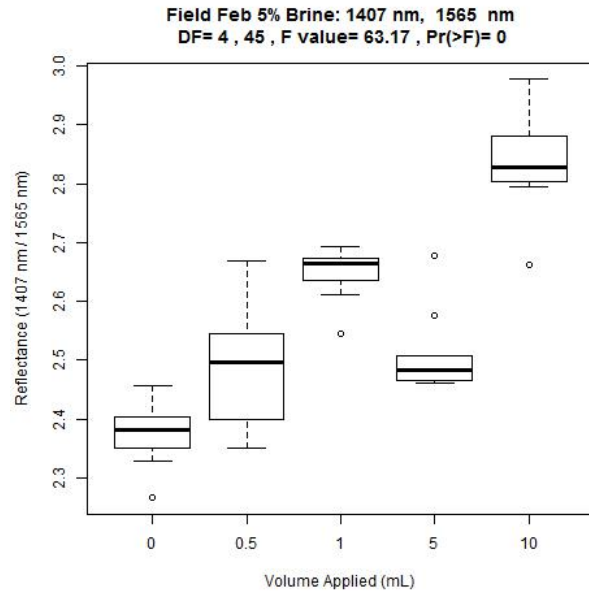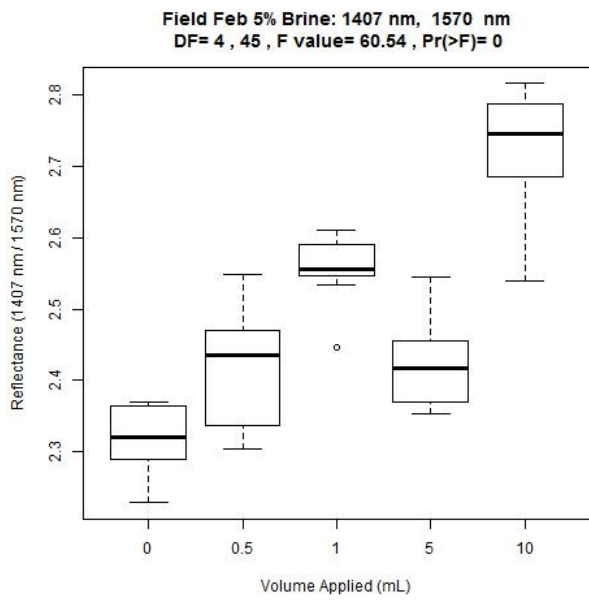
compared, as shown in figure 4.6.

(a)

(b)

(c)

(d)

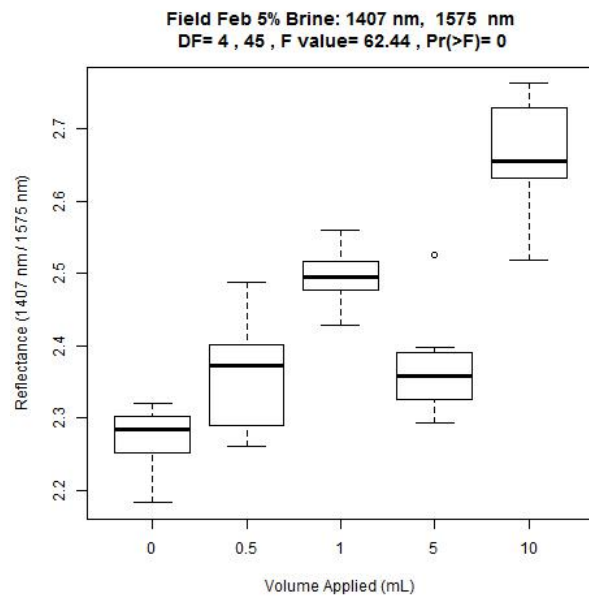**Figure 4.4** 10-mL application, field well-maintained pavement (a) through (d)

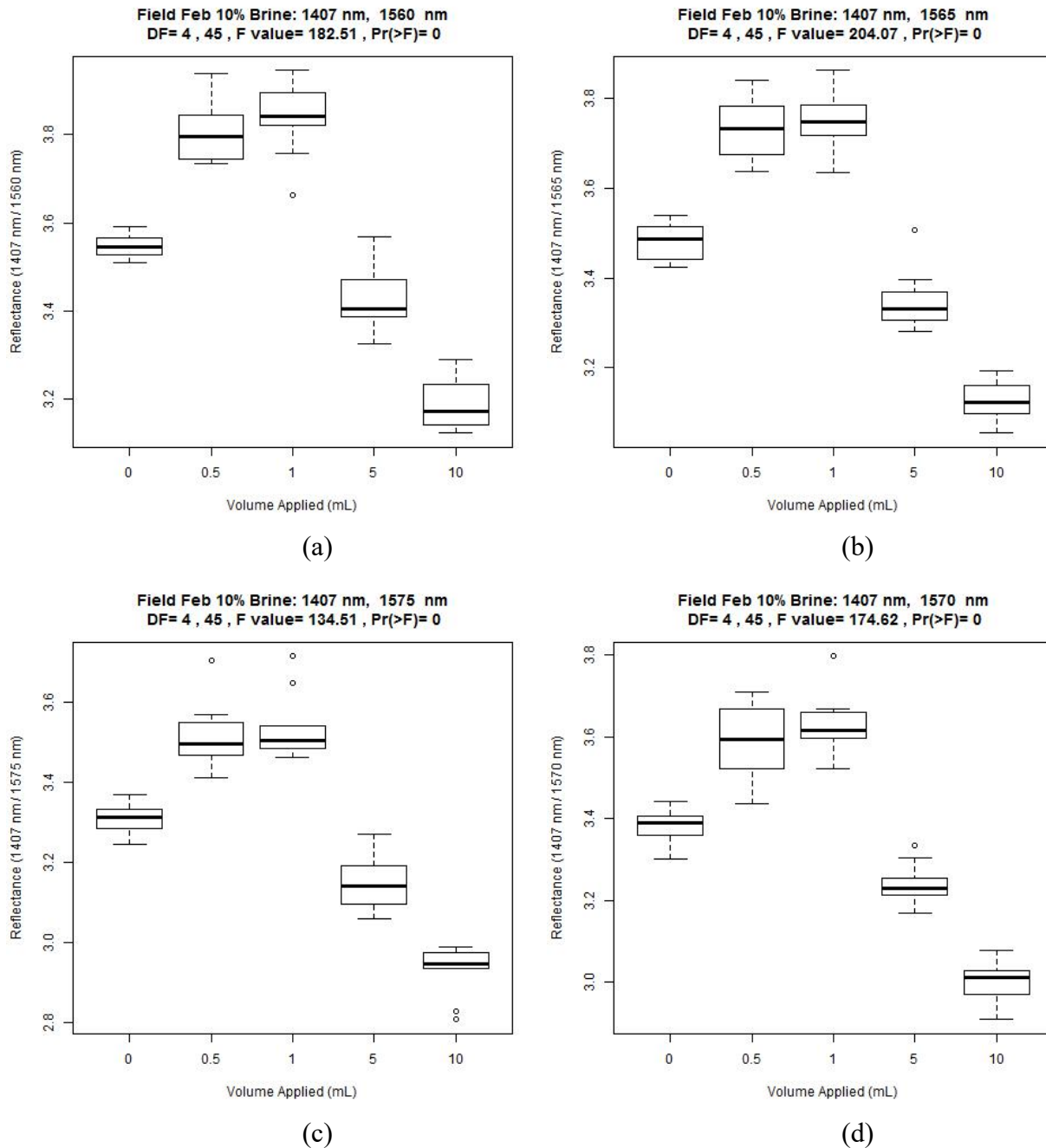Figure 4.5 5 percent concentration application, field well-maintained pavement (a) through (d)

Field Feb 10% Brine: 1407 nm, 1560 nm
DF= 4 , 45 , F value= 182.51 , Pr(>F)= 0

(a)

Field Feb 10% Brine: 1407 nm, 1565 nm
DF= 4 , 45 , F value= 204.07 , Pr(>F)= 0

(b)

Field Feb 10% Brine: 1407 nm, 1575 nm
DF= 4 , 45 , F value= 134.51 , Pr(>F)= 0

(c)

Field Feb 10% Brine: 1407 nm, 1570 nm
DF= 4 , 45 , F value= 174.62 , Pr(>F)= 0

(d)

Figure 4.6 10 percent concentration application, field well-maintained pavement (a) through (d)

An ANOVA test comparing 1407 nm to 1560 nm showed that there was a statistically significant difference between concentrations of deicing compound [$F(4,45) = 182.51$, $p < 0.001$]. Conducting a pairwise comparison with t-tests showed that all the different concentrations were statistically significantly different, except for the 0.5-mL 10 percent brine in

comparison to the 1-mL 10 percent brine compound with *p = 0.39*. Increasing the concentration

of deicer applied should theoretically magnify this trend, which is demonstrated in
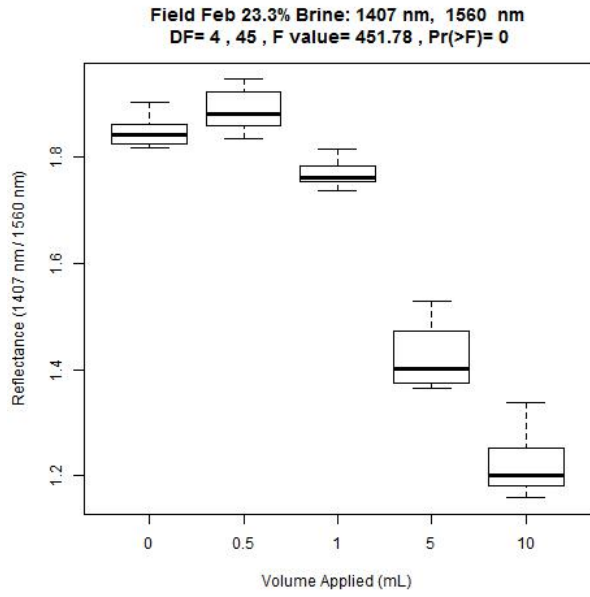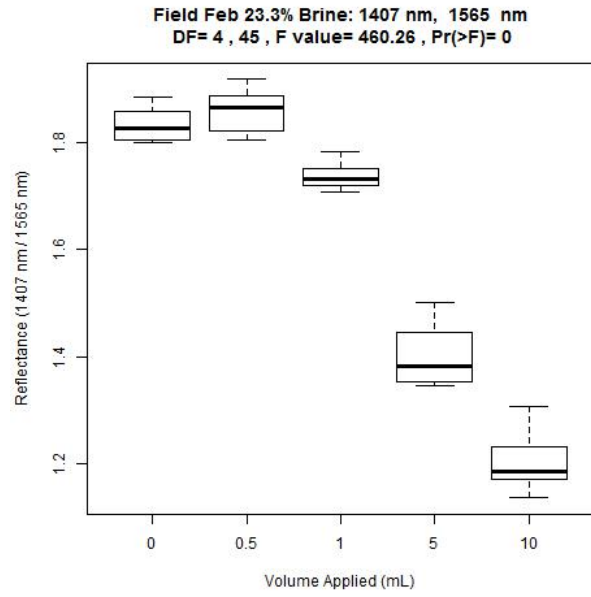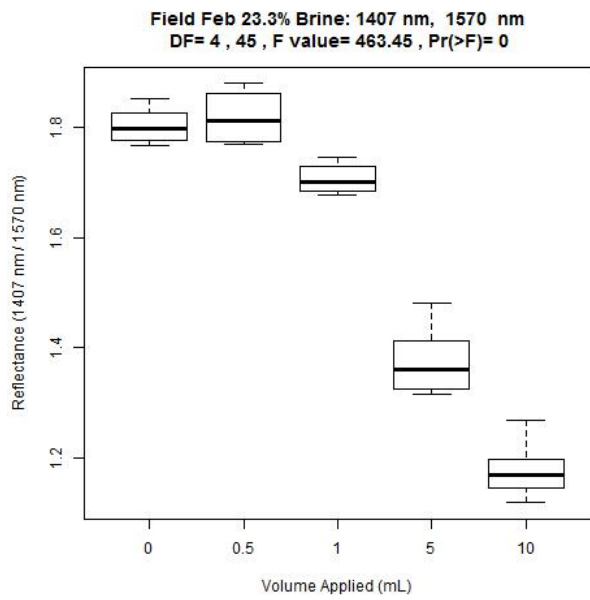
figure 4.7.

(a)

(b)

(c)

(d)
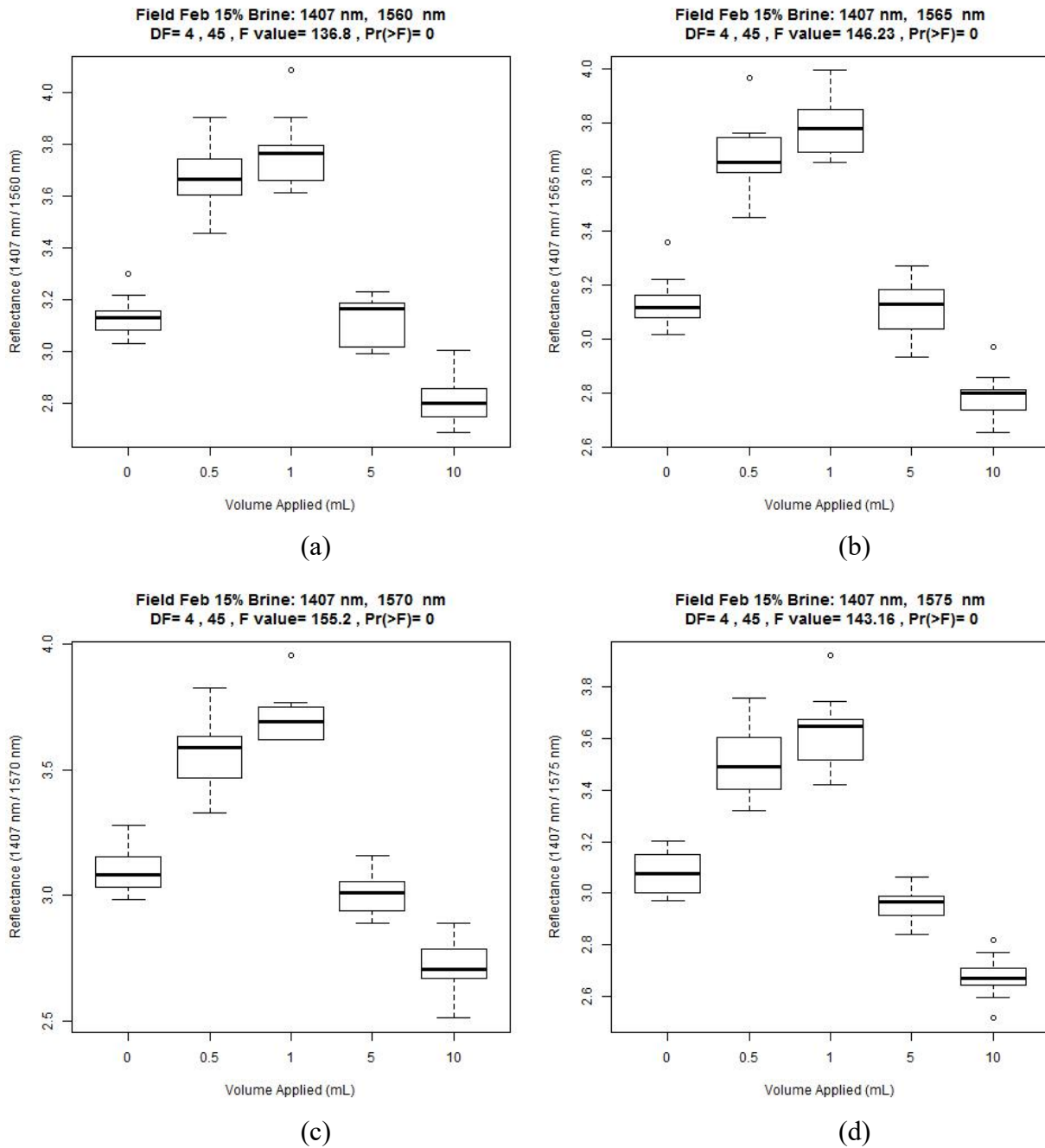
Figure 4.7 15% Concentration Application Field Well-Maintained Pavement (a) through (d)

The highest concentration tested in the field setting was the 23.3 percent brine application shown in figure 4.8. An ANOVA test for this concentration comparing 1407 nm to 1560 nm showed that there was a statistically significant difference between concentrations of deicing compound [$F_{(4,45)} = 136.8$, *p < 0.001*]. Conducting a pairwise comparison with t-tests showed that most concentrations were statistically significantly different, except for the 0.5-mL 15 percent brine in comparison to the 1-mL 15 percent brine compound with a *p = 0.15,* and the 0-mL 15 percent brine in comparison to the 5-mL 15 percent brine compound with a *p = 0.69*.

An ANOVA test comparing 1407 nm to 1560 nm showed that there was a statistically significant difference between concentrations of deicing compound [$F_{(4,45)} = 451.78$, *p < 0.001*]. Conducting a pairwise comparison with t-tests showed that all concentrations were statistically significantly different. The relationships indeed strengthened as the amount applied increased, with 0 mL and 0.5 mL being the only volumes that exhibited no statistical difference, while statistical differences were present for the remainder of the volumetric application rates.
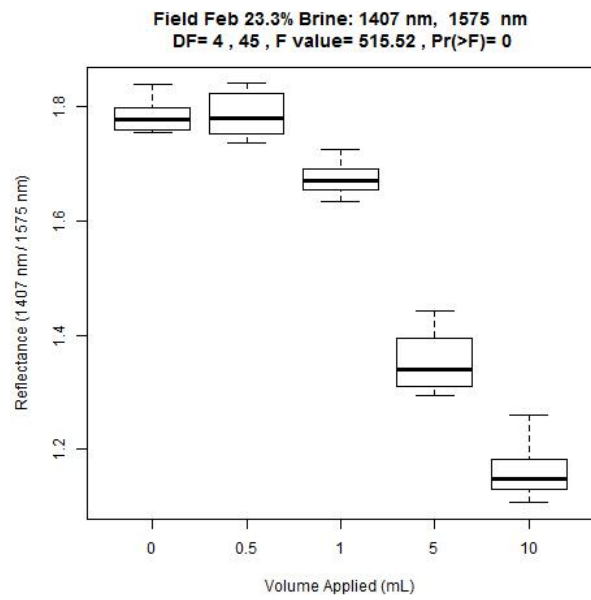
Figure 4.8 23.3 percent concentration application, field well-maintained pavement (a) through (d)

4.10 Beet-Brine

The backgrounds for the beet-brine applications, much like those of the brine applications, were a source of inconsistency in reflectance values for relationship comparisons. Because this uncertainty could possibly have resulted from ice formations, surface striations, or other inconsistencies, the backgrounds were normalized to solidify trends. Background comparisons are shown in figure 4.9.

Analyses at the lowest beet-brine application rate recorded in the field (0.5 mL per 6-inch-diameter area) are shown in figure 4.10. The 0.5-mL application at the maximum concentration was slightly below the maximum rate applied by AKDOT&PF, with the smallest concentration representative of a typical solution.

An ANOVA test comparing 418 nm to 850 nm indicated a statistically significant difference between concentrations of deicing compound [$F_{(4,45)} = 1032.16$, $p < 0.001$]. Conducting a pairwise comparison with t-tests showed that all the different concentrations were statistically significantly different, apart from the 10 percent brine, 8.6 percent beet mixture and the 5 percent brine, 4.3 percent beet mixture, which had $p = 0.64$. The trend was expected to be continuous, with higher concentration applications producing lower reflectance values. However, this trend was not recorded. Instead, there was a sharp dip at 15 percent, brine 12.9 percent beet followed by a resurgence and much larger spread at 23.3 percent brine, 20 percent beet. This was quite different from the lab experimentation results, and the suspected cause was a combination of the elements that were no longer held constant in the field setting, most predominately initial background reflectance. The variation may have been caused by the differences in background, perceptible only on a hyperspectral level, and the associated normalization done to correct the

differences. The effects of doubling the volumetric application to 1-mL application over a 6-inch-diameter area are shown in figure 4.11.
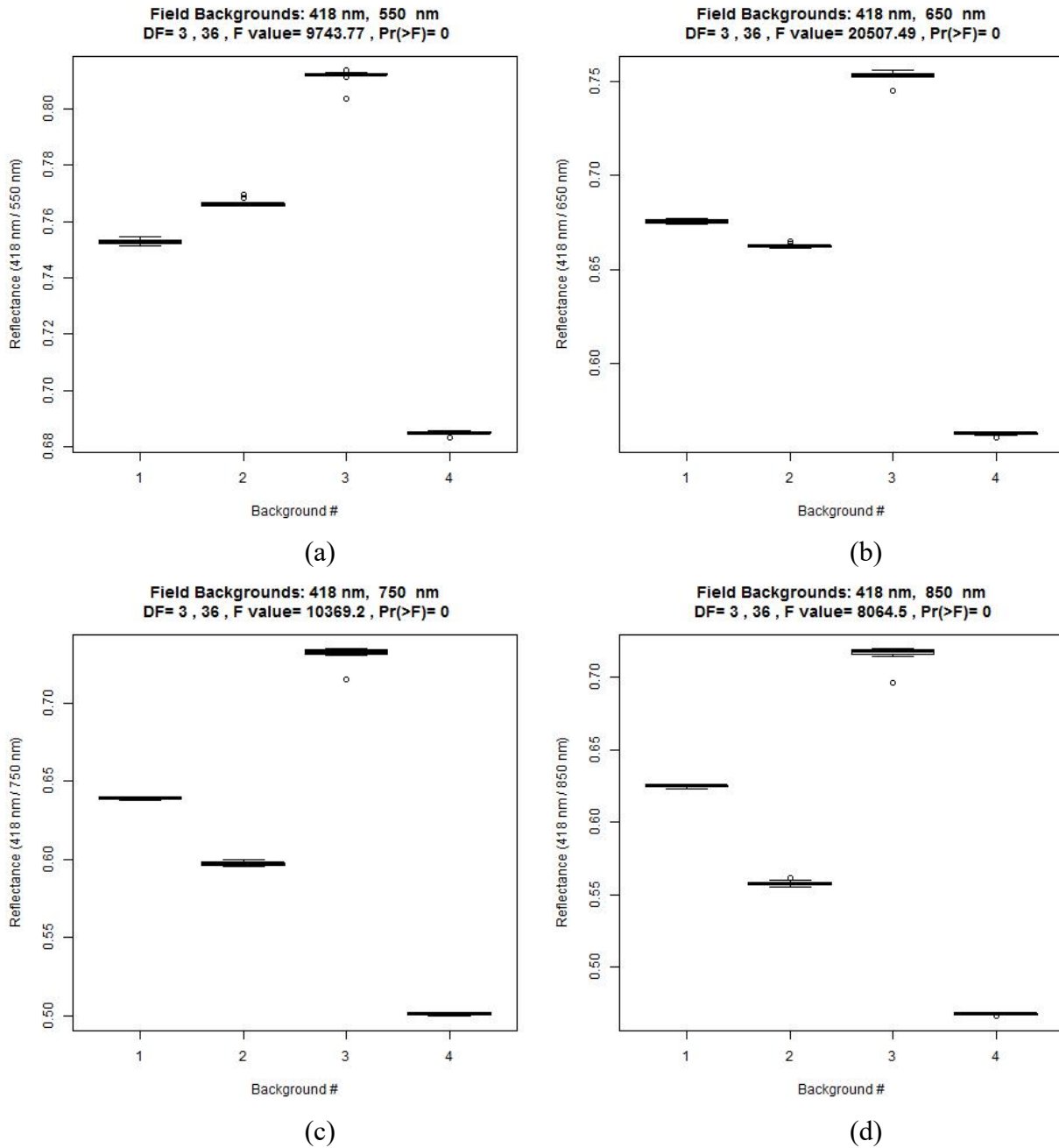

(a)

(b)

(c)

(d)

Figure 4.9 Good condition asphalt pavement, beet-brine background (a) through (d)
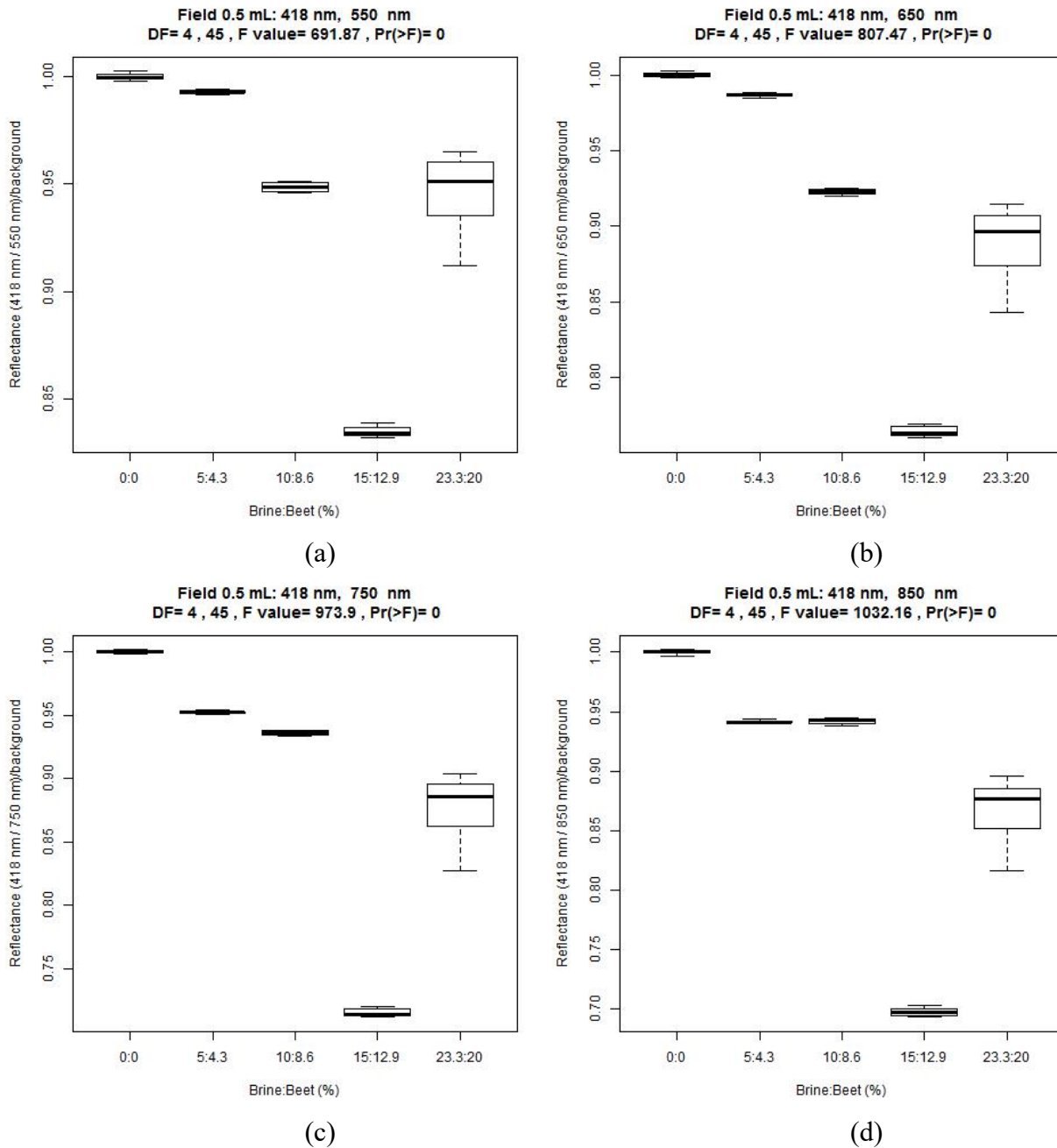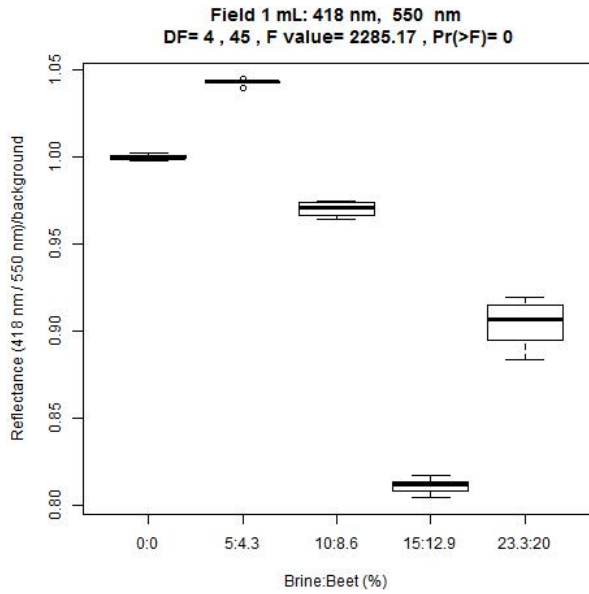
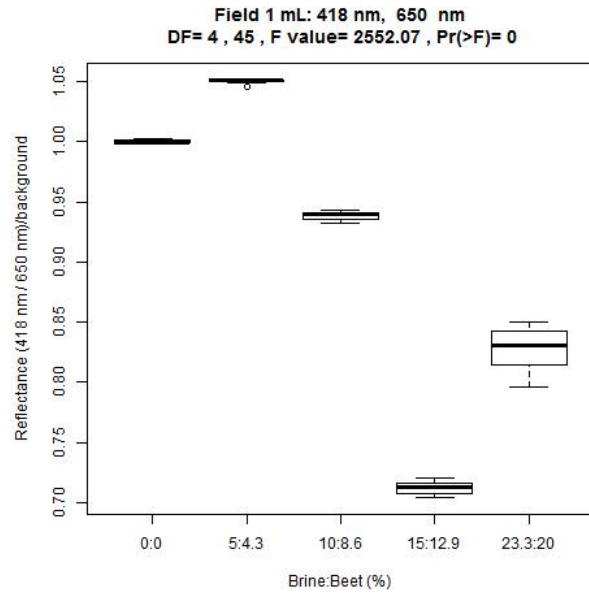**Figure 4.10** 0.5-mL beet-brine, field well-maintained pavement (a) through (d)

A comparison of the 418-nm to 850-nm wavelengths resulted in a statistically significant difference [$F(4,45) = 2508.4$, *p < 0.001*]. The pairwise comparison indicated that all the different concentrations were statistically significantly different. However, the trend among the reflectance values as concentrations increased seemed to deteriorate even though the volumes of

the applications increased. The result of 5 percent brine, 4.3 percent beet solution having a higher reflectance value than its background was not seen at higher wavelength comparisons, such as 418 nm compared to 1050 nm. At these higher values the trends shown in figure 4.11 were mirrored. Further increasing the volumetrics to 5 mL per 6-inch-diameter area would theoretically increase the relationships demonstrated in the boxplots. The results are shown in figure 4.12.

A comparison of the 418-nm to 850-nm wavelengths resulted in a statistically significant difference [$F_{(4,45)} = 119.43$, $p < 0.001$]. Conducting a pairwise comparison with t-tests showed that the majority of different concentrations were statistically significantly different, except the 5 percent brine, 4.3 percent beet solution in comparison to the 23.3 percent brine, 20 percent beet solution with a $p = 0.06$ and the 10 percent brine. 8.6 percent beet solution in comparison to the 23.3 percent brine, 20 percent beet solution with a $p = 0.26$. This lack of statistically significant difference likely stemmed from the wider range of reflectance values. A problem that developed as the application rates approached values exponentially larger than the AKDOT&PF prescribed amount was compound migration. This was especially true with higher concentrations, which is shown by the increasing boxplot size as concentrations increased. At a 5-mL application of 23.3 percent brine, 20 percent beet, the chemicals migrated swiftly off the application site because of melting, uneven asphalt pavement, and the surface pattern of the asphalt pavement.
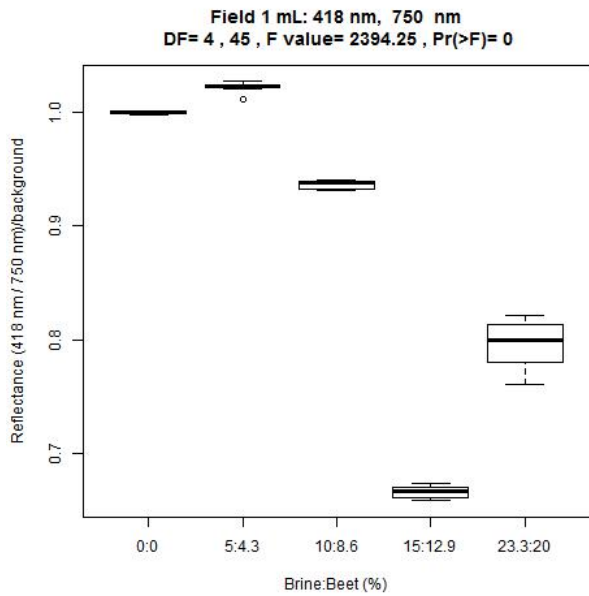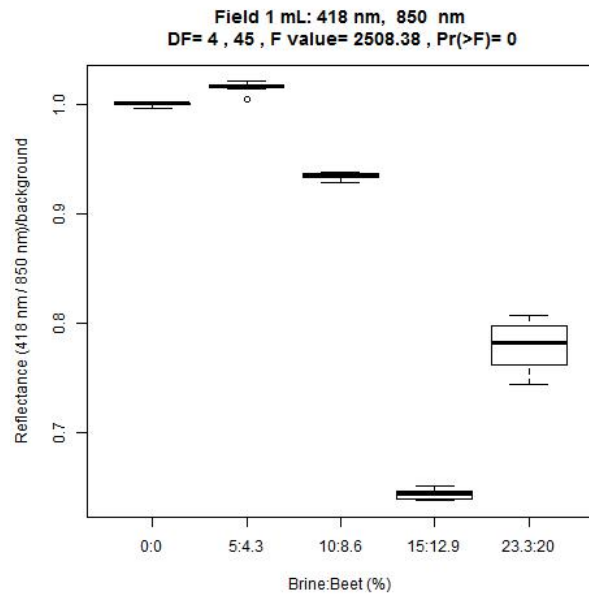
(a)

(b)

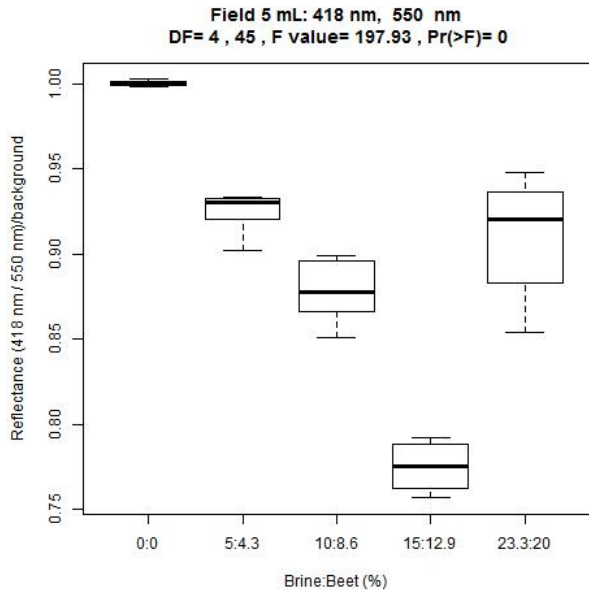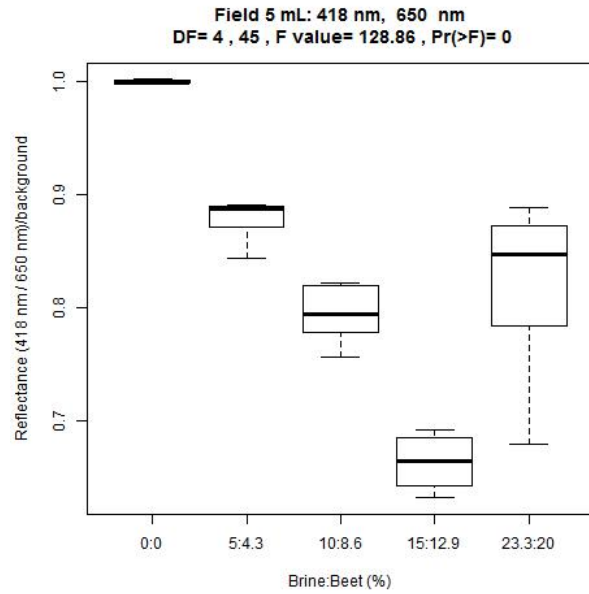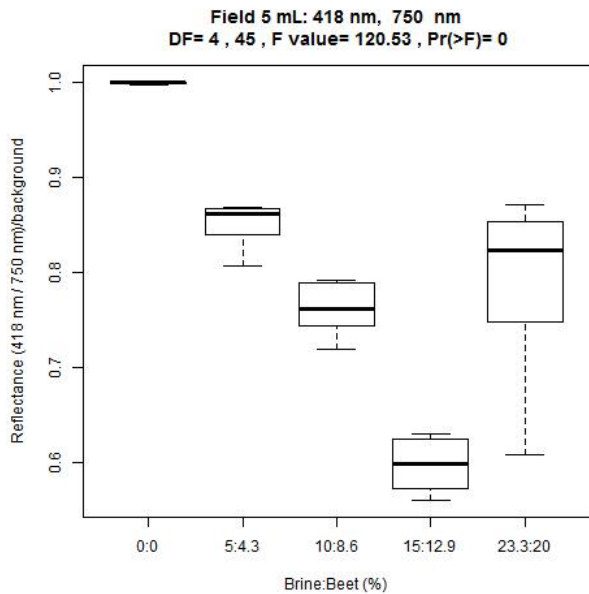**Figure 4.11** 1-mL beet-brine, field well-maintained pavement (a) through (d)

(c)

(d)

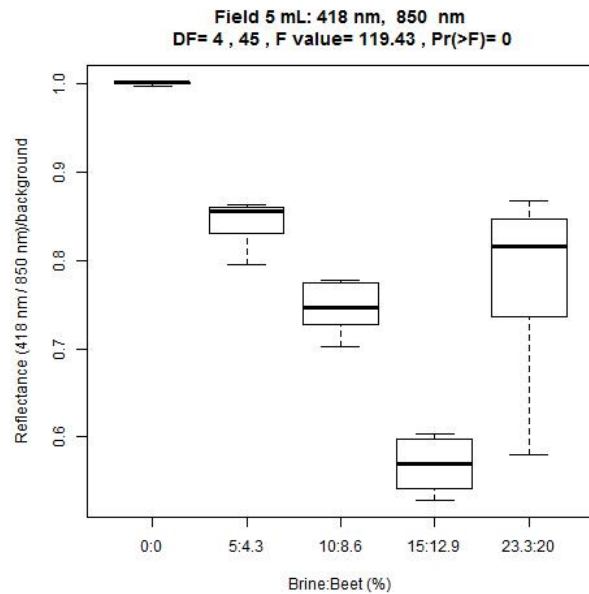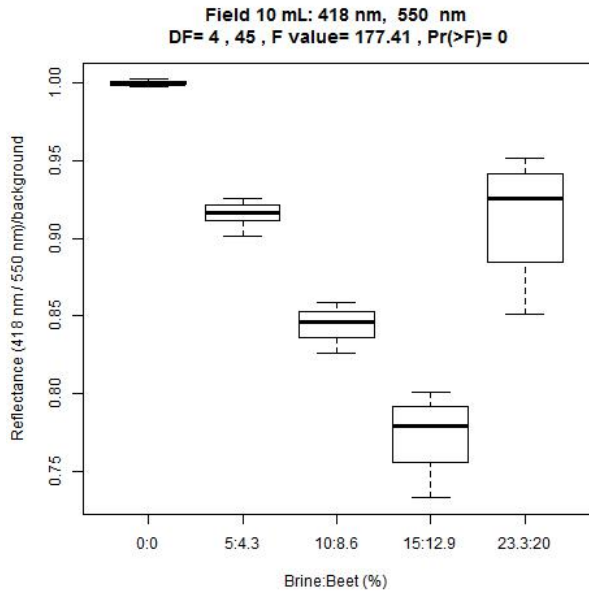**Figure 4.12** 1-mL beet-brine, field well-maintained pavement (a) through (d)

Figure 4.13 5-mL beet-brine, field well-maintained pavement (a) through (d)
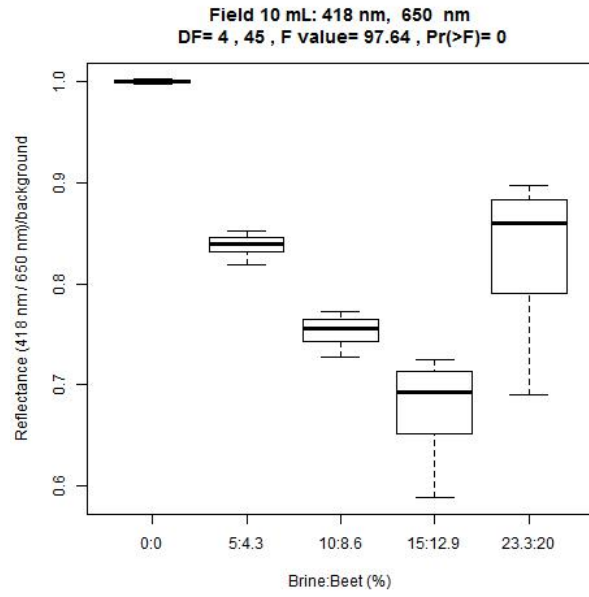
The highest volumetric amount in the field was 10 mL applied over a 6-inch-diameter

area, which was equivalent to about two-thirds the thinnest film thickness recordable in the lab.

At 10-mL applications, too much of the solution was leaving the site, and thicker applications

would not be sustainable. The boxplots are shown in figure 4.13. A comparison of the 418-nm and 850-nm wavelengths resulted in a statistically significant difference [$F_{(4,45)} = 86.17$, $p < 0.001$]. Conducting a pairwise comparison with t-tests showed that all of the concentrations were statistically significantly different, except the 5 percent brine, 4.3 percent beet solution in comparison to the 23.3 percent brine, 20 percent beet solution with $p = 0.80$. The trend continued from previous iterations of field analyses with the 15 percent brine, 12.9 percent beet solution and 23.3 percent brine, 20 percent beet solution having even wider ranges of reflectance values, likely because of increased material migration.
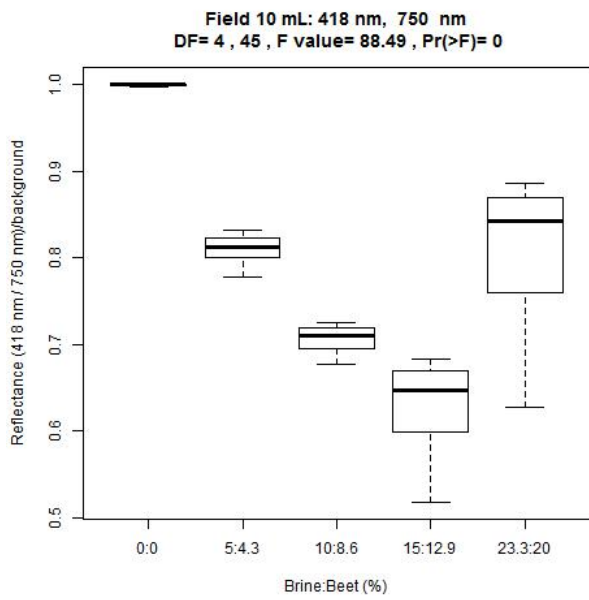
To better control the effects of changing background, the materials were compared with changing volumes but at a constant concentration. The comparisons began with the weakest concentration and increased starting with the 5 percent brine, 4.3 percent beet solution, as shown in figure 4.14. Instead of comparing different concentrations of the same applied volume, different volumes of the same concentration were compared to each other, as shown below in figure 4.15. A comparison of the 418-nm to 850 nm wavelengths resulted in a statistically significant difference [$F_{(4,45)} = 193.42$, $p < 0.001$]. Conducting a pairwise comparison with t-tests showed that all the concentrations were statistically significantly different.
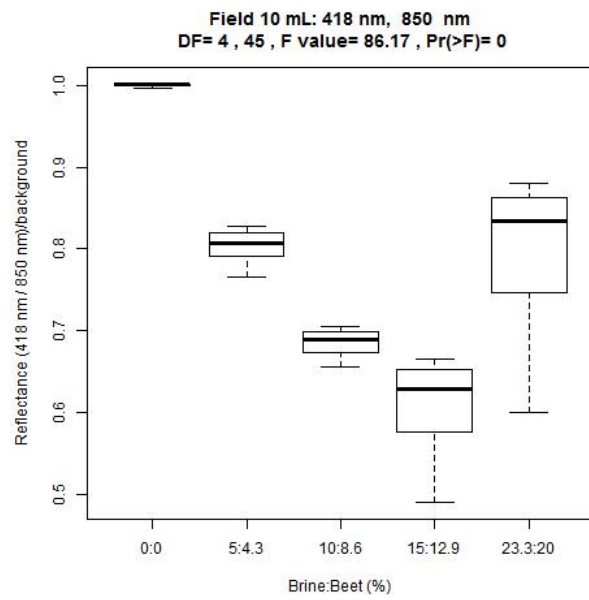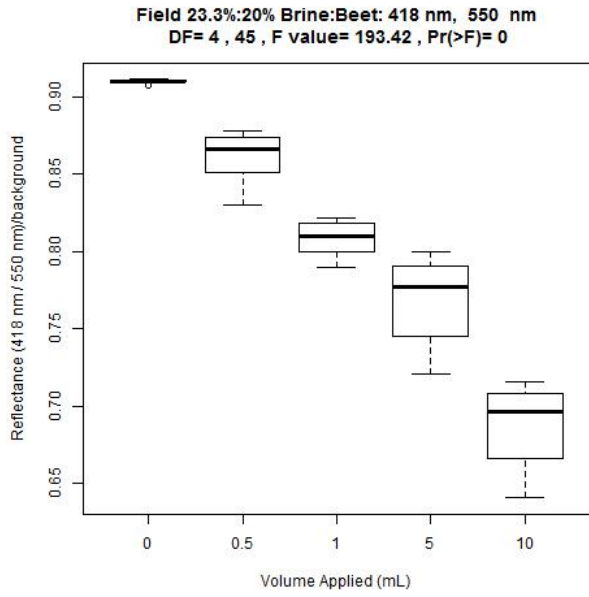
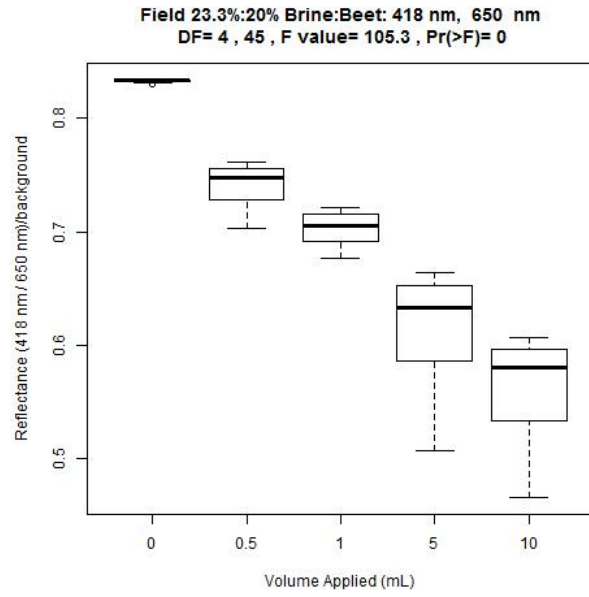**Figure 4.14** 10-mL beet-brine, field well-maintained pavement (a) through (d)

Field 23.3%:20% Brine:Beet: 418 nm, 550 nm
DF= 4 , 45 , F value= 193.42 , Pr(>F)= 0

(a)

Field 23.3%:20% Brine:Beet: 418 nm, 650 nm
DF= 4 , 45 , F value= 105.3 , Pr(>F)= 0

(b)

Field 23.3%:20% Brine:Beet: 418 nm, 750 nm
DF= 4 , 45 , F value= 86.39 , Pr(>F)= 0

(c)

Field 23.3%:20% Brine:Beet: 418 nm, 850 nm
DF= 4 , 45 , F value= 74.8 , Pr(>F)= 0
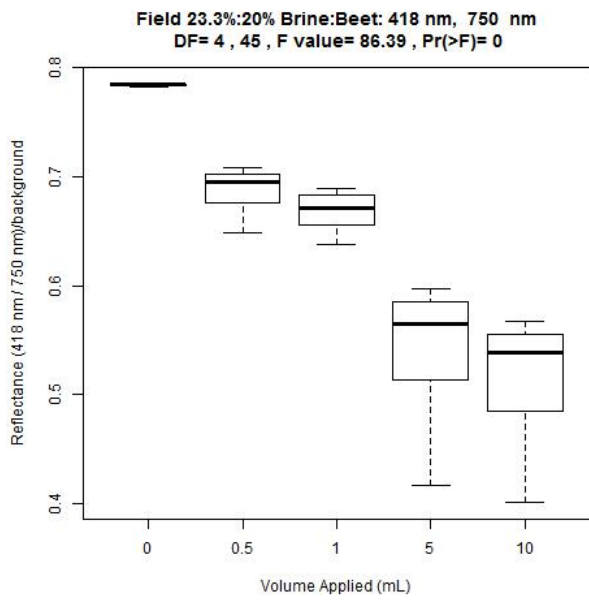
(d)

Figure 4.15 23.3 percent brine, 20 percent beet application, field well-maintained pavement (a) through (d)
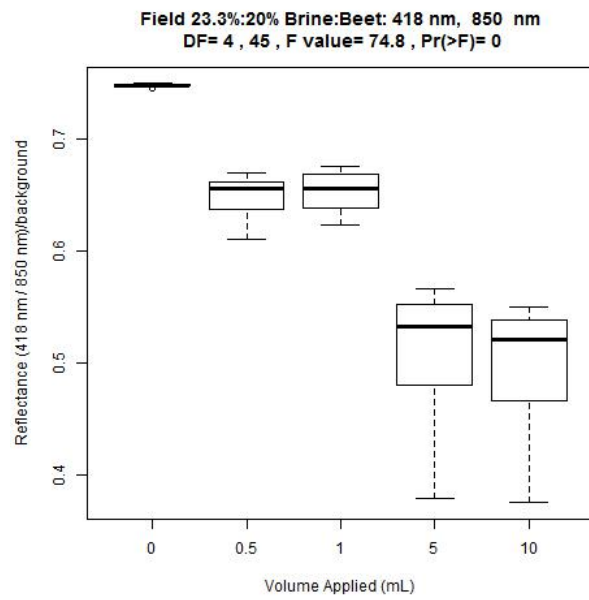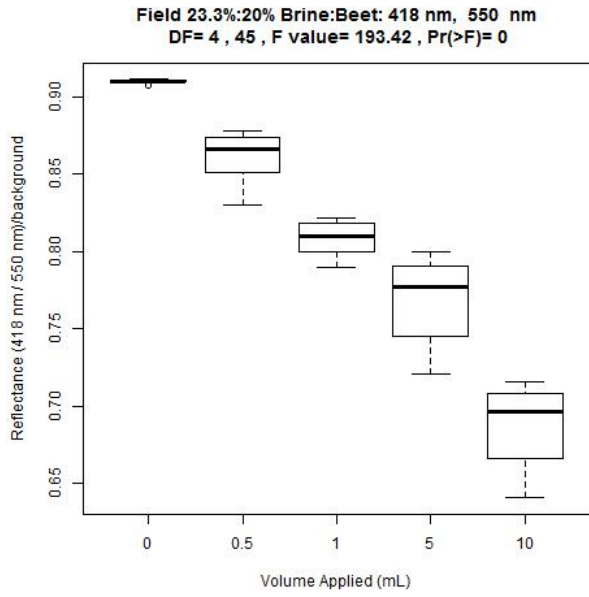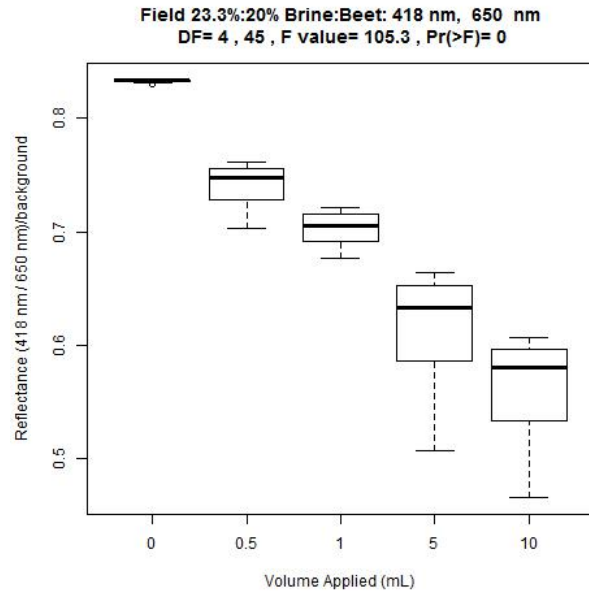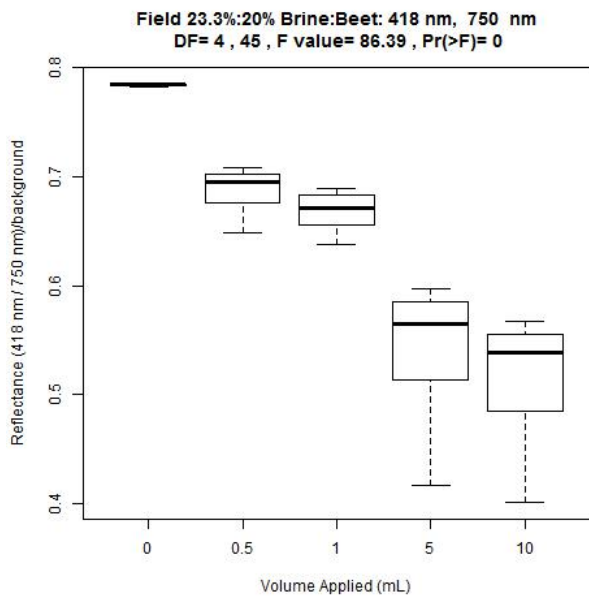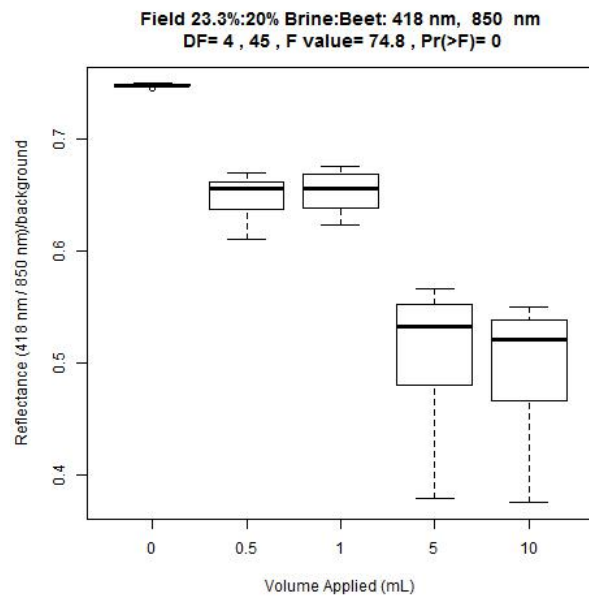
(a)

(b)

(c)

(d)

Figure 4.16 23.3 percent brine, 20 percent beet application, field well-maintained pavement (a) through (d)

Chapter 5 Discussion and Conclusions

The goal of this research project was to explore the feasibility of establishing relationships that could represent the presence and concentration of deicing materials applied to winter roads by utilizing spectral imaging hardware in a field setting. To that end, the methods and data generated for this project represent progress in the development of an objective method to detect and quantify chlorides and related solutions in near-real time for roadway environments.

The results and deliverables of this research demonstrated broader applicability of hyperspectral sensing technologies in the field of transportation. The findings of this research serve to quantify the amount and nature of imposed loss of anti-icing and deicing chemicals and might provide information that can be used to better inform winter maintenance efforts and activities. This will improve the efforts of DOTs and other municipalities to effectively manage and mitigate the effects of winter precipitation events. In turn, this will directly improve the winter mobility of our highway systems. Follow-on research activities could include the inclusion of hyperspectral imaging units at existing RWIS sites for real-time monitoring and feedback of anti-icing and deicing efficacy to support current MDSS efforts. This project was the second phase of a larger study that focused specifically on field-based data and how to extend the methods developed in Phase 1 into a less-controlled environment that must consider and account for several environmental factors.

Testing and exploration of the effectiveness and repeatability of lab-based relationships developed in Phase 1 in a field- and in-situ-based based environment highlighted the limitations of the hyperspectral equipment, as well as revealed some conditions for which the band math relationships initially developed in the lab were valid.

A major difficulty experienced in this research was the deleterious effects of water on NIR wavelengths. As the deicing chemical accomplished its purpose, the melting ice turned to water and began to pool on the application site. At certain thicknesses, types, and conditions, water and ice have extremely low reflectance values (i.e., ice and water absorb light and can prevent the identification of other materials contained in solution). Adding salt to water to make a brine results in absorption features and decreased reflectance in the NIR range, either making it impossible to see or massively muting the key brine signatures.

The approach that promised the highest likelihood of success was to select the points that had the highest rate of repetition, theoretically representing the wavelengths that would exhibit the greatest sensitivity to changes in concentration and volume. The wavelengths that had the highest number of matching points to their curve that produced a linear trend were then statistically analyzed. Relationships that proved to be highly accurate in a lab setting showed some issues when applied to data gathered in the field. For brine, low concentrations and low volumetric applications tended to have a positive trend (counter to lab-based data from Phase 1), whereas higher application rates tended to have a negative trend that matched data gathered in the lab. The lowest application rates from Phase 1 were higher than the field setting's highest application rate. While not an unreasonable expectation, the hope was that the relationships established in the lab would be strong enough to detect accurate field concentration readings, regardless of the volume applied to the surface.

The beet-brine relationships from Phase 1 were stronger than brine relationships in the lab setting; the field-based data achieved similar accuracy and consistency. Field data were also subject to several uncertainties related to background variation. Different wear, icing, and overall heterogeneity of asphalt pavement all resulted in different reflectance values, and overall

magnitude caused lateral shifts in the recorded spectra. Normalization was used to rectify these aberrations; however, it was unable to fully control for this error under some conditions. This was possibly due to the complex and variable nature of the crystalline structure of surface ice types, typically imperceptible to the human eye.

This research established that changes in concentration of deicers (specifically brine and beet-brine) can be accurately measured, are statistically significantly different at different concentrations, and have consistent trends in a controlled lab setting as documented in Phase 1. The salt index equation used in soil identification (Asfaw, Suryabhagavan, & Argaw, 2016) was tested again and produced several relationships that were more statistically significant than the initial field method tested.

This research specifically limited its scope to only two variables (i.e., concentration and volume) in the analysis. Future research should focus on field-based data, better controlling for the effects of varied lighting and surface conditions. In addition, focusing on wavelengths that can be acquired through current satellite arrays and multinomial band math could address some of the limitations experienced here.

References

Belz, N.P., Fulton, G. (2019). *Measuring Dispersal and Tracking of Anti-Icing and Deicing Chemicals using In-Situ Spectral Data – Phase 1,* Pacific Northwest Transportation Consortium, Seattle, WA, 88pp. http://hdl.handle.net/1773/45580

Fay, L., M.Sc, Honarvarnazari, M., Ph.D., Jungwirth, S., M.Sc., Muthumani, A., M.Sc., Cui, N., Ph.D., & Shi, X., Ph.d., P.E. (2015, June). Manual for Environmental Best Practices for Snow and Ice Control (Proj.). Western Transportation Institute. http://clearroads.org/wp-content/uploads/dlm_uploads/Manual_ClearRoads_13-01_FINAL.pdf

IHS (2014, February 24). The Economic Costs of Disruption form a Snowstorm Retrieved December 12, 2017, from https://www.highways.org/wp-content/uploads/2014/02/economic-costs-of-snowstorms.pdf

Kuemmel, D. A., & Hanbali, R. M. (1992, June 1). Accident Analysis of Ice Control Operations (Rep.). Retrieved December 13, 2017, from The Salt Institute website: http://www.trc.marquette.edu/publications/IceControl/ice-control-1992.pdf

McClellan, T., Boone, P. and Coleman, M. 2009. Maintenance Decision Support System (MDSS): Indiana Department of Transportation (INDOT) Statewide Implementation, Final Report. Indiana DOT.